We would like to sincerely thank the reviewers for their time efforts in reviewing this manuscript. We believe that the suggestions offered have improved this work. Please find our responses to the comments below.

Reviewer #1

If my guess is right, a majority of modelers who have put their hands on the development of a model of tropospheric bromine chemistry know, sort of heuristically, that the partitioning of inorganic bromine in the troposphere is highly sensitive to heterogeneous recycling (e.g., HOBr + HBr -> Br2 + H2O) in/on the aerosols (see, for example, Yang et al., 2005). So I wasn't surprised too much while reading the present paper by Thompson and co-workers despite the tone of its message. In my opinion, the main value of the present paper is the use of the "radical chain length" as an objective measure. I find it very interesting. That being said, I feel that the authors should revise their discussions and, possibly, even redo their model calculations as detailed below. One of my major concerns is that the authors seem to have precluded much too easily a possibility for the under-representation of heterogeneous reactions in/on the aerosols while discussing the missing source of Br2 in their model calculations. I would recommend the publication of this work in ACP with major revisions.

The reviewer is correct that in our submitted manuscript we implied that the reactions of HOBr on the snowpack was the source of Br_2 (cf. Pratt et al., 2013; Lehrer et al., 2004), while in fact reactions on aerosols could be an important source. In the revision, in multiple places, we now specify that it is a condensed phase process, either involving aerosols and/or the snowpack.

 [Specific comments]

1. For the analysis of the same dataset obtained at Barrow in the spring 2009, Liao et al. (2012) apparently used aerosol physical parameters from in-situ measurements for estimating the rate of HOBr uptake onto aerosols. On the other hand, I cannot find a description of how the present study deals with the aerosol volume and surface area and their temporal variability to constrain the rate of reactions involving aerosols. This aspect needs to be discussed thoroughly before concluding the predominant contribution of the surface snowpack in explaining the levels of Br2 measured in the field.

We in fact cannot quantitatively distinguish between the snowpack and aerosols because of, as we have discussed in the paper, the inability given the current state of scientific knowledge, to simulate snowpack photochemistry, on the basis of fundamentals. Implying that we could was an error, corrected in the revised manuscript. We only state that much or most of the Br atoms are derived from Br_2 photolysis, where most of the Br_2 is produced from the condensed phase (by inference). The revised manuscript now quantifies how much of the Br_2 is likely from condensed phase emissions by considering, and correcting for, the known gas-phase production pathways [Lines 712-722]. Our model was originally developed with the intention of incorporating a full heterogeneous mechanism with both the snow and aerosol parameterized separately based on the model framework of Michalowski et al. (2000). In that work, they used a constant average aerosol surface area of 3.95 x 10^{-7} cm^2/cm^3 from measurements made at Alert

by Staebler et al. (1994), with a maximum aerosol radius of r = 0.1 μm, and this is also what we used. Though we did not use the measurements from Barrow, the value we used is consistent with observations of aerosol surface area at Barrow, which ranged between 9 x 10^{-8} cm^2/cm^3 and 40 x 10^{-7} cm^2/cm^3 (Liao et al. 2012). We have added Lines 293-311 in the revised draft explaining this. However, because we were unable to reproduce observed Br_2 and Cl_2, we opted to forgo all of the heterogeneous production mechanisms (both aerosol and snow), and simply constrain to the observations. The "surfaces" are only important in terms of a sink, and there is no chemistry or production (with the one exception of BrCl, as noted in Lines 275-280). Because of this, we cannot, and do not, attempt to separate Br_2 being produced from aerosols or snow, and instead simply lump these two together as "surface." The use of the word surface perhaps was unclear, therefore we have added a sentence on Lines 307-310 to specifically state this.

2. Observational data for Br2 are apparently missing for the majority of period between March 29-30 (Figure 2A; see also, Liao et al., 2012). Among the entire period of March 25-31 studied here, the period of March 29-30 is quite distinct in that ozone is recovered to near-background levels at 20-30 ppbv, which I understand is important for examining a contrast between ODE and non-ODE conditions. I suggest the authors to comment on the unavailability of Br2 data between March 29-30, how they have managed to fill in this data gap and what it means to the completeness of their model-assisted analysis. I also feel that the time series in Figures 2, 3, 5, 6, 7, 8A and 9 should be marked to indicate that the Br2 measurements were missing during March 29-30.

We have added discussion in the Methods section (Lines 268-275 of the revised draft) addressing the missing Br_2 observations and explaining how this period was filled in based on the observations of the adjacent days. Our estimation of Br_2 during this data gap results in BrO values in good agreement with observations, therefore, we believe the estimations to be reasonable. In all of the figures in the revised manuscript presenting analyses from the model (new Figures 3,5-10), we have indicated the period of missing Br_2 values with a shaded box.

3. Any explanation for apparently much higher short-term variability in simulated BrO (black line) than in-situ measurements (red dots), especially during March 29-31, in Figure 2B? Although not necessarily relevant, it is during this period of time that disagreement between modeled and measured HOBr becomes really bad.

The higher short term variability is a result of reading in (unsmoothed, but sub-sampled) atmospheric datasets from a variety of instruments that all have their own inherent noise associated with the measurements, which is then compounded through multiple chemical reaction calculations. This variability is not important to the conclusions of the modeling, since we look at daily trends in the data, and it is a distraction that unnecessarily complicates the figures. Therefore, we have opted to smooth the model output using hourly averages and have implemented this in all figures. With regard to HOBr, we have revised the model so that we now constrain to the HOBr observations. This doesn't impact the conclusions of the paper since HOBr is important only as a photolytic precursor to Br atoms.

4. Lines 299-318 (Chain lengths defined by Method 1 & Method 2): I believe, "J_BrONO2 * [BrONO2]" should be taken away from the numerator of the Method 1 formula. It should also be moved from the numerator to the denominator in the Method 2 formula.
According to the authors' definition, BrONO2 is the product of a termination reaction (hence k * [BrO] * [NO2] is in the denominator of the Method 1 formula). If these are not simple typographic errors, the authors should recalculate the chain lengths with corrected formulae.

This is correct, thank you. This correction has been applied to the equations, and all values recalculated, with the figures updates accordingly.

5. Line 346-348: If the authors rationalize the exclusion of the photolysis of organobromine compounds from the chain initiation term (denominator) in Equation (6), there's not much point for including the OH-attack on CH3Br and CHBr3 instead. I would have liked the formula better if the authors had included all the following terms in the denominator of Equation (6): J_BrONO2 * [BrONO2], J_BrNO2 * [BrNO2], J_CHBr3 * [CHBr3] and k * [HBr] * [OH].

Regarding the organobromine reactions, this is a fair point. Both the OH reactions and photolysis are negligible terms. Following this suggestion, however, we have added bromoform photolysis to Equation 6, as well as $BrONO_2$ photolysis, $BrNO_2$ photolysis, and HBr + OH, and stated Lines 454-463 of the revision that these are present in the interest of completeness.

6. I would like to see plots equivalent to Figures 6-7 for the chain initiation. How dominant is the photolysis of Br2 in there?

This is a very good suggestion. We have added a figure (new Figure 6) showing the time-varying rates for the initiation reactions. In Panel A, it is clear that Br_2 photolysis far dominates the initiation. In Panel B, we have removed the Br_2 photolysis term so that the other initiations can be seen. Lines 562-588 of the revised manuscript have been added to discuss this new figure.

7. The role of BrO + HO2 followed by the photolysis of HOBr in the net loss of ozone has been already recognized to be relatively important in the context of chemistry in the springtime polar boundary layer (Piot and von Glasow, 2008, see their introduction; Hausmann and Platt, 1994; Sander et al., 1997). In particular, Hausmann and Platt (1994, section 5 and Fig. 8) and Sander et al. (1997, section 3.1 and Fig. 2) conducted some useful calculations that can be compared with the analysis performed in the present study. Therefore, the discussion of the role of BrO + HO2 should start from Section 3.4 on ozone loss rate (rather than Section 3.5) where Figure 8 could be expanded to include additional lines and dots with contributions from k*[BrO]*[HO2] added to 2*(k*[BrO]^2 + k*[BrO]*[ClO]). And the authors should refer to those two earlier studies at first and then explain what is new and perhaps different in the present study.

Our reason for using the $2(k[BrO]^2 + k[BrO][ClO])$ estimation is because this method has been used in several previous works to estimate the O_3 loss rate and, as such, has been accepted to be a valid estimation. We show that this method accounts for only 44% of the ozone loss rate, and that estimating O_3 loss with only BrO observations is inaccurate, which is one of the new outcomes of our study. To address this suggestion, however, we have now added to this figure (new Figure 9B) an estimation for O_3 loss using only $k[BrO][HO_2]$ (as done in Hausmann and

Platt, 1994, Figure 8) and also an estimation combining all 3 of these gas-phase cycles. Consistent with Hausmann and Platt, 1994, Figure 8, the O_3 loss rate estimated by $k[BrO][HO_2]$ is much slower than even $2(k[BrO]^2 + k[BrO][ClO])$ and only accounts for 18% of the O_3 loss rate. Combining the 3 gas-phase cycles gives an estimation that is faster, but still only accounts for 60%. We have added this discussion in the text in Section 3.4 Lines 660-675 of the revised manuscript.

In regards to Sander et al. (1997), Figure 2, we have added discussion in Section 3.5, Lines 694-707 comparing our results for the $BrO + HO_2$ reaction rate to that calculated by Sander et al. Our reaction rate is much faster than that of Sander, and we consider that this is likely due to the large differences in HO_2 mixing ratios between our models.

Then, in Section 3.5, the authors must clarify how much of HOBr thus generated ends up in heterogeneous reactions on the aerosol and snow surfaces rather than photolysis in the gas phase.

Because we cannot accurately simulate heterogeneous chemistry in the snowpack component of the model, and because of the very large uncertainties associated with any estimation of HOBr deposition velocities to either snow or aerosol, we could not address this using our model with any sort of accuracy. Thus, as stated above, we chose to constrain the model to HOBr observations. This, of course, makes addressing this question completely impossible. In order to address this question, then, we ran another version of our model with a variable surface deposition, based on daily wind speeds, that was tuned to achieve reasonable agreement with observations. This is discussed in Lines 355-371, and new Figure 2 has been added to show the difference in HOBr between these simulations. Using the simulation with the variable HOBr deposition, we were able to estimate that 19% of HOBr is lost to photolysis and 80% is lost to "surfaces" (some combination of aerosol and snow). The low contribution of HOBr photolysis to Br initiation is consistent with Zeng et al. (2006). This point has been added to the text in Section 3.3, Lines 579-588, where we discuss the initiation terms.

Also, it seems useful to mention the dominance of Br + HCHO as a source of HO2 (Thompson et al., 2015) under the conditions of the air studied here and what it means to the contributions of BrO + HO2 to the ozone loss and the heterogeneous formation of Br2 and BrCl in the snow and the aerosols.

We have included lines 699-701 of the revised manuscript, stating this pathway as a primary source of HO_2, in the discussion of the $BrO + HO_2$ reaction rate comparison with Sander et al. (1997). Even at the higher HO_2 levels encountered at Barrow, in comparison to the Sander et al. results, the $BrO + HO_2$ gas-phase cycle is a minor contributor to ozone depletion, and so would be even less so with lower HO_2. We do not simulate heterogeneous production of Br_2, so we cannot address what impact this would have on Br_2 production in our model. As a thought experiment, one could reasonably argue that to a first approximation lower HO_2 values would lead to lower HOBr, which would in turn decrease heterogeneous Br_2 production (and vice versa). This is an interesting question, but not one that we can address with our specific model.

The role of aerosol uptake in controlling the HOBr mixing ratios has been discussed using the same dataset from Barrow by Liao et al. (2012), which should be referred to and discussed in the context of the present study.

We have added further discussion of this aspect of the Liao et al. (2012) study to the Methods section in Lines 304-307, and also to the new discussion of Figure 2 (showing HOBr in different simulations) on Lines 358-363.

8. Are the aqueous-phase (or surface) reactions of BrNO2 and BrONO2 with halide anions in aerosols and snow grains included in the model? I don't see them in Table 1, but they could be rather important at high levels of NOx such as on March 25.

These aqueous phase reactions are not included because we do not produce Br_2 or Cl_2 through the heterogeneous mechanism. We do include deposition of these species to the surface as a sink term following the same method as in Custard et al., 2015 (however, we have noticed that these deposition terms were not included in Table 1, and we apologize for that oversight). Without these sink terms, the mixing ratios of $BrNO_2$ and $BrONO_2$ predicted by the model become very high, thus they are included, but no chemistry is done with them once they deposit. The photolysis of $BrNO_2$ as a bromine atom initiation source is relatively higher on March 25 (see new Figure 6), but this still does not compete with Br_2. As is mentioned in the Methods section, only BrCl is produced through the (admittedly simplistic) heterogeneous chemistry, and the mixing ratios of 0-10 pptv are consistent with the relatively sparse BrCl observations that we do have from Barrow. BrCl is not a significant factor in bromine initiation compared to Br_2.

9. Although I understand it useful to refer to a possible involvement of iodine photochemistry, there is no unequivocal evidence for its strong contributions at Barrow as much as assumed in the "High Iodine" scenario. Since, despite its hypothetical nature, this topic has been addressed once in their earlier paper (Thompson et al., 2015), I suggest the authors not to stress it much too strongly in the present paper. For example, the first paragraph of Section 3.3 may indeed need a brief comment on the hypothetical nature of the "High Iodine" scenario.

This is a good suggestion and we agree. For this paper, we have now omitted the High Iodine scenario altogether, instead using only the more realistic Low Iodine scenario. Iodine is now only addressed in Table 2 and Figure 5 in terms of chain length, and in Figure 7 in terms of potential for bromine propagation.

10. Line 229: Here, the first-order rate constant of transfer out of the snowpack of emitted species is referred to as the same as the first-order rate constant of transfer of depositing species from the air to the snowpack. But this seems odd, considering a large difference in assumed volumes between the air (the entire boundary layer) and the snowpack.

The mass transfer in and out of the snowpack was made equivalent in the same manner as Michalowski et al. (2000), which assumes that the mass transfer is limited only by the rate of vertical mixing. However, mass transfer is only important for the depositing species for surface sink terms since we do not produce Br_2 or Cl_2 heterogeneously, thus, there is in effect no mass transfer out of the snowpack.

11. Line 402: Looking at the NOx data presented in Custard et al. (2015), NOx appears to have been pretty high on March 26 as well.

There are sporadic enhancements in NO_x through the late morning of March 26, but were not seen from mid-day onwards. The main difference between NO_x on March 25 and March 26 is that NO_x was continuously enhanced on the 25th with concomitant continuous enhancement of CO, whereas on the 26th there were only sporadic and short-lived spikes of NO_x that did not display the same CO enhancements. For the NO and NO_2 values that were read into the model, they were subsampled at 10 minute intervals, which eliminated the short transient spikes on the morning of 26 March. Because they were transients, and not correlated with CO, we do not consider them to have a large impact on the chemistry. The figure referred to in Custard et al. (2015) was produced by smoothing all of the data by averaging, such that those transients skewed the smoothed data upwards.

12. Lines 468-470: This finding is not new; the authors should read Barrie et al. (1988, page 140), Zeng et al. (2006, equation (2) and paragraph [15]) and Holmes et al. (2010, equation (2)).

We have revised the tone of this statement and acknowledge that this has been previously recognized and applied to the Br steady state calculations presented in Zeng et al. and Holmes et al.

13. Lines 496-497: Cite Bottenheim et al. (1990) along with Shepson et al. (1996) when referring to the role of CH3CHO as a sink for Br-atom.

This has been corrected, as suggested by the reviewer.

14. Lines 599-601: There are no actual model results presented in this paper regarding the role of snow gain acidity in the Br2 surface fluxes. This statement should be dropped; otherwise, cite the model study of Toyota et al. (2014), which have demonstrated the role of pH in the snow QLL in the production of Br2 using a condensed phase chemical mechanism similar to the one employed in the present study.

We have dropped these lines from the text, and also have cited the modeling studies of Toyota et al. 2011 and 2014 in our mention of the pH of the QLL, Lines 777-781 of the revision.

[Technical suggestions]

1. Throughout the manuscript, the authors use the nomenclature "mole ratio" when referring to what is normally called "mixing ratio" or "mole fraction" in atmospheric chemistry. I suggest the authors to use either of the latter two.

We have changed all of these instances to mixing ratio.

2. Explain what the J-max is (Line 200) – a theoretical daily maximum under the clear sky? Also, how are the J-values are scaled under cloudy conditions? A sentense or two will do.

We have added lines 234-238 text stating that "All other photolysis reactions were scaled to $J(NO_2)$ in the modeling code using the maximum J coefficients (J_{max}) for 25 March (a clear-sky day) as a scaling factor. For cloudy days, this method assumes that J coefficients for other photolytically-active species are attenuated in a manner that is proportional to $J(NO_2)$."

3. Line 209: . . . using this mechanism; however, . . .

This has been corrected.

4. Table 1: It appears that the mass transfer of HCl between gas and condensed phases should be included, as it is probably important for the formation of BrCl in the aerosols.

This has been added to Table 1.

Reviewer #2

This paper uses a 0D box model with a simplified description of heterogeneous chemistry to study the cycle of bromine during ozone depletion events and non-ozone depletion conditions in Barrow, Alaska. This paper is interesting because it proposes to use the bromine chain length to study the relative importance of gas phase cycling of bromine compared to primary emissions/heterogeneous recycle of bromine, both of which have long been thought to be important for catalytic ozone destruction by bromine in the Arctic boundary layer. Upon a first look, the paper appears to be well thought out and presented resulting in some interesting conclusions. But, upon deeper scrutiny it is clear there are some major problems with the modeling approach that need to be addressed. In its current form, the paper does not meet the standards for publication in ACP. The paper may eventually be considered for publication, but major modifications to the modeling approach and conclusions are required.

The main problem is that the model in its current state make it impossible to answer the questions proposed by the authors. How can the authors compare chain cycling with primary emissions, when they don't model either primary emissions or heterogeneous recycling of halogens on aerosols? In their model, Br2 is fixed to the measured concentrations (not formed by processes in the model) therefore, there is a contribution from some unknown source or sink of Br2 (and hence 2Br) at each time step of the model. Another way to think about this is to ask the question – how can the authors distinguish heterogeneous chain propagation to form Br2 from surface emissions of Br2? Using the current model setup, these cannot be distinguished making the analysis of the chain length and comparison to primary emissions rates derived incorrect.

What we can do, and did explain more clearly in the revision, is calculate what fraction of Br atoms are derived from gas phase radical reactions vs. from emissions from the condensed phase. The latter can indeed be from aerosols or from the snowpack. We cannot distinguish, because as stated on pages 11 and 12 of the revision, it is not possible to accurately simulate snow phase photochemistry. It is thus true that by constraining the model to Br_2 observations we cannot inherently say how much of the observed Br_2 is from surfaces and how much is from gas-phase reactions. To address this, in Section 3.3 and the new Figure 6, where we discuss the initiation reactions, we make clear that the Br_2 photolysis includes all Br_2. In the original Section 3.5 where we had determined Br atom production from "surface emissions", we had assumed that all Br_2 was from the surface. We have now modified that to correct for Br_2 produced in the gas-phase by creating a proxy in the model, Br_2^*, that is Br_2 formed only in gas-phase reactions. Thus, by subtracting Br_2^* from Br_2, we get our best estimate for Br_2 that is from condensed phase chemistry. This has also allowed us to determine that, on average, Br_2 produced via gas-phase reactions can account for 35% of the observed Br_2. Lines 708-722 of Section 3.5 in the revision have been added to discuss this.

It is also important to understand that the chain length refers only to gas-phase radical reactions, and by definition, does not include heterogeneous reactions, and our lack of knowledge of the details of heterogeneous chemistry has no impact on this analysis. We have attempted to make this point clearer in the text.

There are further warnings of serious problems for using this modeling approach to understand how BrO + BrO competes with primary emissions of Br2 (or heterogeneous recycling of HOBr to Br2). These include:

1. The measured concentrations of BrO and HOBr are not actually captured by the model (Figure 2, 30 & 31 March). Given this, the regime where BrO + BrO dominates cannot be studied adequately.

We have now constrained our model to the observations of HOBr, and have added a new Figure 2 to the revision. The new BrO values are shown in Figure 1. Constraining HOBr slightly decreased BrO. The variability of the modeled output has also now been smoothed with hourly averaging (see response to Reviewer 1, comment 3). With the constrained HOBr, the model now explicitly represents HOBr observations, and we feel that the modeled BrO is also in good agreement with the observations.

2. The model over predicts very high HOBr concentrations (Figure 2, 30 & 31 March), leading to the conclusion that there may be something wrong with their heterogeneous uptake and recycling to Br2 of HOBr. This also limits the ability of the model to compare/contrast Br2 formed in the gas phase with Br2 formed via heterogeneous chemistry.

As discussed, we chose to constrain the model to HOBr observations, since we cannot simulate the snowpack photochemistry. We did, however, also run a version of the model with variable HOBr deposition, based on daily wind speeds, that was tuned to better reproduce the observations. This is shown in new Figure 2C in the revision. This version of the model was used to determine that 19% of HOBr is lost to photolysis and 80% is lost to surfaces (some

combination of snow and aerosol). All other calculations (e.g. the chain length, and relative sources of Br atoms) were redone using the model constrained to HOBr. Because we also constrain to Br_2, our model does not inherently separate Br_2 from surface emissions and Br_2 from gas-phase reactions. For this reason, we incorporated our gas-phase Br_2 proxy, Br_2*, as discussed above.

3. Equation 9 is extremely misleading – attributing all Br2 photolysis to surface emissions. Br2 is also the product of the BrO + BrO self-reaction. Br2 formed from BrO+BrO in the gas phase must also be considered in this equation and throughout the paper when discussion the Br chain length.

We agree that assuming all Br_2 is from the surface (as was done in Equation 9) is inaccurate. Therefore, we have now corrected that equation (new Equation 10), by subtracting Br_2 formed via gas-phase reactions (Br_2*) from the total observed Br_2. Thus, new Equation 10, now represents our best estimate for Br_2 from surface emissions from the condensed phase (aerosol + snowpack). By doing this, we were also able to determine that gas-phase production of Br_2 accounts for 35% on average of the observed Br_2. The source of the Br_2 has no impact on the chain length calculation, however, as the photolysis of Br_2 (regardless of source) is an initiation term for Br. That said, in discussion of the new Figure 6, where we show the rates of the initiation terms, we do now point out clearly that the Br_2 photolysis term includes all Br_2 regardless of source [Lines568-570].

4. There is no mention of the prior work by Toyota et al. (2014, 2011) on the importance of surface recycling for HOBr to sustain ozone depletion events/bromine release. These modeling papers should be referenced and fully discussed. References to other modeling work on this topic is also missing and should be more thoroughly discussed/thought through.

References to Toyota et al. (2011, 2014) have been added to both the Methods and the Results sections.

5. There is no discussion of the role of HOBr formation (XO + HO2) and subsequent photolysis in bromine recycling. This is a major problem, given its role in chain propagation.

This comment was also made by Reviewer 1. We have addressed this in several ways following the suggestions by Reviewer 1. We have added a new Figure 6, which shows the bromine initiation terms and demonstrates the minor role of HOBr photolysis for bromine initiation. Here, we also now discuss that we have found that photolysis accounts for 19% of the HOBr loss and surface deposition accounts for 80%, based upon our model simulation with variable and enhanced HOBr deposition (Figure 2C). This minor role of HOBr photolysis is consistent with the work of Zeng et al. (2006). Additionally, in discussing the O_3 loss rates in Section 3.4, we have added O_3 loss rate estimations using $k[BrO][HO_2]$, comparing to a similar calculation by Hausmann and Platt (1994), further confirming the minor contribution of this gas-phase pathway.

6. Do the authors propose to separate primary emissions (bromine explosion initiation step) from emissions on snow/aerosols via HOBr recycling?

We do not propose to separate Br_2 that is emitted from the surface in the initial bromide activation step (the mechanism for which is not fully understood, though several theories do exist) versus Br_2 that is emitted from the surface following HOBr recycling. Indeed, this work does not provide any information about the chemical mechanism that produces Br_2 from the condensed phases. In referencing "primary emissions", we were simply referring to any Br_2 that is emitted from a surface through any mechanism. Equation 9 (new Equation 10) has been updated and recalculated to correct for Br_2 formed through gas-phase pathways (such as one channel of the BrO + BrO reaction), so that the result of this equation is our best estimate for Br atoms derived from Br_2 that was produced in a condensed phase. Here, "condensed phase" refers to some combination of aerosol and snow.

7. There is no discussion of the role of heterogeneous recycling of BrNO3. The paper cannot be considered for publication without heterogeneous recycling through BrNO3 uptake included in the model.

As we have discussed, we are not simulating heterogeneous chemistry. We have expanded the discussion in the Methods section to make this clearer and to justify why we chose not to produce these compounds heterogeneously, citing the works of Domine et al. 2013 and Cao et al., 2014, which clearly discuss the inherent difficulties in attempting to model snow surface chemistry. Indeed, these papers argue that snow surface chemistry cannot be modeled accurately at this time given the state of our knowledge. Deposition of $BrONO_2$ (and $BrNO_2$) is included as a sink term in the same manner as in Custard et al. (2015). We regret that these deposition terms were overlooked in Table 1 and that has been corrected. As discussed, the chain length refers to gas phase radical chain propagation only, and therefore it is important to understand that explicit heterogeneous reactions have no bearing on this metric.

8. Given the high NOx levels at Barrow, a thorough discussion (including figures that demonstrate that nitrogen oxides are adequately modeled) is needed. The role of chain recycling through NOx must be considered and discussed.

The impact of NO_x on the bromine chain length is discussed in Lines 487-506, and is discussed in much greater detail in Custard et al. (2015). Custard et al. also address the role of NO_x in moderating the rate of ozone depletion. Because this is the main topic of that work, we don't feel that we need to expand further in this current manuscript and restate the conclusions of Custard et al. To the extent that NO_x impacts recycling via $BrNO_2$ and $BrONO_2$, again, we don't/can't simulate that chemistry in the snowpack. Our model is constrained to NO and NO_2 observations and this figure is shown in Thompson et al. (2015).

9. Given the nature of surface emissions from snow, which are the main focus of the conclusions, there are likely to be vertical gradients in the concentrations of both nitrogen and bromine containing species. What are the implications of ignoring these vertical gradients on the conclusions regarding the chain length compared to primary surface emissions?

This is a very good point, and we have added Lines 762-777 in the Conclusions section addressing this. The lines we have added state:

"We find that between 30 – 90% of Br atoms are produced from surface emissions of Br_2 and BrCl, though we cannot distinguish snow sources from aerosol sources using our model. However, it is important to note that we do not know how much of the condensed phase Br_2 production derives from reaction R7, or from some other condensed phase process, e.g. oxidation of Br^- by OH radicals (Abbatt et al., 2010). The in situ snow chamber experiments by Pratt et al. (2013) demonstrate a strong Br_2 source from the snowpack; similar field observations proving significant Br_2 emissions from Arctic aerosol are currently lacking. If the snow surface is the primary sources of these emissions, then a strong vertical gradient would be expected in the near surface boundary layer, and our estimations for the Br chain length would be only valid for the height of our measurements (~ 1 m above the snow). Strong deposition to the snow would also induce a vertical gradient in these species. If, however, aerosols are an important source of Br_2 (or other halogen precursors), then Br_2 production should occur throughout the entire height of the boundary with no significant vertical gradient, in a similar fashion as has been observed for $ClNO_2$, which is a known product of aerosol chemistry (Young et al., 2012). It is clear that vertically-resolved measurements of these halogen precursors are imperative for our understanding of halogen production in the Arctic."

10. Are the model rate constants independent of temperature as suggested by Table 1? If there is no temperature dependence of rate constants included, the model is likely wrong during portions of the day as many of the reaction rates depend on temperature and the surface temperature at Barrow has an important diurnal cycle during this portion of the year.

Most of the rate constants involved in radical recycling are indeed not very temperature dependent. We feel that this is justified in this case because ambient temperature in Barrow for the week of 25 March 2009 varied by less than 10 K between the maximum and minimum recorded daily temperatures. Also, the radical oxidation and radical-radical reactions that are of primary importance here do not have a large dependence on temperature (Atkinson et al., 2006, 2007); for example, a variability of 10 K imposes an ~1% change on the rate of ethane oxidation by Cl atoms and a <4% change on the rate of the BrO + BrO radical self-reaction. Furthermore, and as mentioned previously, the major stable chemical species driving the model, especially those VOCs that can exhibit a more important temperature dependence, are highly constrained to observations and are not allowed to freely evolve. We have added text to the Methods section Lines 202-213 addressing this point.

The paper cannot be published in the current format. The heterogeneous reactions involved in halogen recycling are not thoroughly discussed/considered in chain propagation. The most recent halogen review papers have more clear discussions of these radical cycles (e.g. Abbatt et al., 2012). There is also a clear discussion of these cycles in earlier reviews, for example Monks et al. (2005).

The chain length, by definition, is a metric for the radical chain propagation in the gas phase only, and as such, does not include heterogeneous reactions. As an example, the work by Monks et al. (2005), which we do cite in reference to the chain length, also uses the chain length metric to discuss the gas-phase cycling of HOx. The implication of a short gas-phase chain length is that bromine recycling through the heterogeneous reactions is highly important, but again, this cannot

be accurately simulated on the basis of fundamentals. While previous modeling studies do show that bromine production cannot be sustained without heterogeneous chemistry, we are using a specific metric, the gas-phase chain length, to support the conclusions of those works and argue that the rate of ozone depletion cannot be accurately estimated with gas-phase reactions alone, as has been done in several papers.

The authors have done some modeling work that can potentially be extended to answer questions about the relationship between bromine cycling and ozone depletion events. However, with their current model the authors cannot adequately compare the bromine chain length with primary emissions using a 0D chemical box model setup that relies on fixing the essential radical precursors to measurements. The authors should consider a major revision that answers a set of scientific questions that are appropriate for the model they use.

Minor comments:

1. Figure 1 is already found in Thompson 2015 (Figure 1a). Is there a specific reason for it to be included as a separate figure here? The ozone time series can simply be added to what is now Figure 2.

Figure 1 and 2 have been combined. The ozone time series is now shown as Panel A in Figure 1.

2. The authors should mention in their reaction schemes (equations listed) that HOBr also reacts to OH + Br in the gas phase.

The photolysis of HOBr to OH + Br is listed in Table 1, as is the reaction of HOBr with OH.

1 **Bromine atom production and chain propagation during springtime Arctic ozone depletion**

2 **events in Barrow, Alaska**

3

4 Chelsea R. Thompson,[1,a,b] Paul B. Shepson,[1,2] Jin Liao,[3,a,b] L. Greg Huey,[3] Chris Cantrell[4,c],

5 Frank Flocke[4], and John Orlando[4]

6

7 [1]Department of Chemistry, Purdue University, West Lafayette, IN, USA
8
9 [2]Department of Earth and Atmospheric Sciences and Purdue Climate Change Research Center,
10 Purdue University, West Lafayette, IN, USA
11
12 [3]School of Earth and Atmospheric Sciences, Georgia Institute of Technology, Atlanta, GA, USA
13
14 [4]National Center for Atmospheric Research, Boulder, CO, USA
15
16 [a]now at: Cooperative Institute for Research in Environmental Sciences, University of Colorado
17 Boulder, Boulder, CO, USA
18
19 [b]now at: Chemical Sciences Division, NOAA Earth System Research Laboratory, Boulder, CO,
20 USA
21
22 [c]now at: Department of Atmospheric and Ocean Sciences, University of Colorado Boulder,
23 Boulder, CO, USA
24

25 *Correspondence to:* C. R. Thompson (chelsea.thompson@noaa.gov)
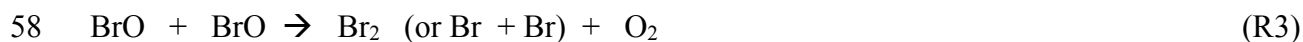
26

27

28 **Abstract.** Ozone depletion events (ODEs) in the Arctic are primarily controlled by a bromine

29 radical-catalyzed destruction mechanism that depends on the efficient production and recycling

30 of Br atoms. Numerous laboratory and modeling studies have suggested the importance of

31 heterogeneous recycling of Br through HOBr reaction with bromide on saline surfaces. However,

32 the gas-phase regeneration of bromine atoms through BrO-BrO radical reactions has been

assumed to be an efficient, if not dominant, pathway for Br reformation and thus ozone destruction. Indeed, it has been estimated that the rate of ozone depletion is approximately equal to twice the rate of the BrO self-reaction. Here, we use a zero-dimensional, photochemical model, largely constrained to observations of stable atmospheric species from the 2009 OASIS campaign in Barrow, Alaska, to investigate gas-phase bromine radical propagation and recycling mechanisms of bromine atoms for a seven-day period during late March. This work is a continuation of that presented in Thompson et al. (2015) and utilizes the same model construct. Here, we use the gas-phase radical chain length as a metric for objectively quantifying the efficiency of gas-phase recycling of bromine atoms. The gas-phase bromine chain length is determined to be quite small, at <1.5, and highly dependent on ambient O_3 concentrations. Furthermore, we find that Br atom production from photolysis of Br_2 and BrCl, which is predominately emitted from snow and/or aerosol surfaces, can account for between 30 – 90% of total Br atom production. This analysis suggests that condensed phase production of bromine is at least as important as, and at times greater than, gas-phase recycling for the occurrence of Arctic ODEs. Therefore, the rate of the BrO self-reaction is not a sufficient estimate for the rate of O_3 depletion.

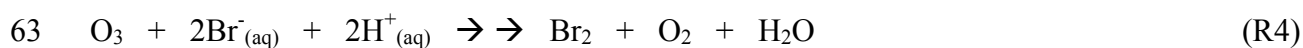## 1 Introduction

The springtime depletion of boundary layer ozone in the Arctic has been the subject of intense research for several decades. Early observations revealed a strong correlation between ozone depletion events (ODEs) and enhancements in filterable bromine (Barrie et al., 1988). This discovery led researchers to propose a mechanism for the bromine-catalyzed destruction of ozone.

56    $Br_2 + h\nu \rightarrow 2Br$ (R1)

57    $Br + O_3 \rightarrow BrO + O_2$ (R2)

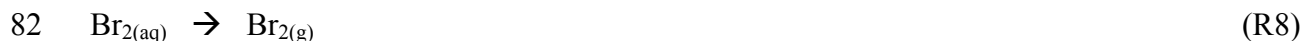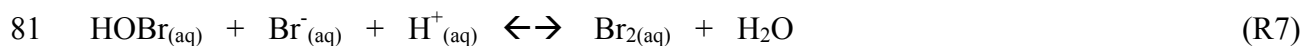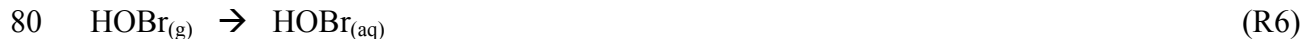58 $BrO + BrO \rightarrow Br_2$ (or $Br + Br$) $+ O_2$ (R3)

59   This reaction cycle requires an initial source of bromine atoms to the boundary layer. Laboratory

60   and theoretical studies have suggested that Br_2 could be produced through oxidation of bromide

61   present in salt-enriched snow, ice or aerosol surfaces by gas-phase ozone (Hirokawa et al., 1998;

62   Oum et al., 1998b; Gladich et al., 2015).

63    $O_3 + 2Br^-_{(aq)} + 2H^+_{(aq)} \rightarrow\rightarrow Br_2 + O_2 + H_2O$ (R4)

64   Field observations by Pratt et al. (2013) using a controlled snow chamber experiment with

65   natural tundra snow collected near Barrow, AK lend further evidence to this mechanism, and

66   also suggest Br_2 production from OH produced photochemically within the snowpack. This

67   mechanism was further explored in the modeling study of Toyota et al. (2014) that suggested an

68   important role for this activation pathway in producing bromine within the snowpack interstitial

69   air.

70   Once present in the gas-phase, bromine atoms can be regenerated through radical-radical

71   reactions of BrO with XO (where X = Br, Cl, or I), NO, OH, or CH_3OO to propagate the chain

72   reaction and continue the destruction cycle of ozone. If BrO photolyzes or reacts with NO, O_3 is

73   regenerated, and there is a null cycle with respect to O_3. However, although O_3 is not destroyed,

74   these two pathways represent efficient routes for Br atom propagation. Thus R3 serves to make

75   R2 effective in destruction of O_3. At the same time, Br atoms could be recycled through

76   heterogeneous reactions of HOBr with bromide in the condensed phase to release Br_2 to the gas-

77   phase via the now well-known "bromine explosion" mechanism (Vogt et al., 1996; Tang and

78   McConnell, 1996; Fan and Jacob, 1992).

79      $BrO + HO_2 \rightarrow HOBr + O_2$ (R5)

80      $HOBr_{(g)} \rightarrow HOBr_{(aq)}$ (R6)

81      $HOBr_{(aq)} + Br^-_{(aq)} + H^+_{(aq)} \longleftrightarrow Br_{2(aq)} + H_2O$ (R7)

82 $Br_{2(aq)} \rightarrow Br_{2(g)}$ (R8)

83   Evidence for reaction sequence R5 – R8 has been provided through laboratory studies, which

84   found that Br_2 was produced when frozen bromide solutions were exposed to gas-phase HOBr

85   (Huff and Abbatt, 2002; Adams et al., 2002). This mechanism is believed to proceed rapidly to

86   produce Br_2 so long as sufficient bromide is present in an accessible condensed phase. The

87   efficiency of this heterogeneous recycling mechanism has also been found to have a dependence

88   on the acidity of the surface, as was shown using natural environmental snow samples in Pratt et

89   al. (2013) and investigated in the modeling studies of Toyota et al. (2011, 2014), in a manner that

90   is consistent with the stoichiometry of Reaction R7.

91   To efficiently sustain the ozone destruction cycle to the point of near complete loss of

92   boundary layer ozone ($[O_3] < 2$ ppb), bromine atoms must be continually recycled through some

93   combination of the above mechanisms. The gas-phase reaction cycle described by Reactions R1

94   – R3 has generally been considered to be the dominant pathway for Br reformation following the

95   initial activation of Br_2 from the surface (the mechanism for which is still not fully understood).

96   Thus, it has been assumed that the rate of ozone destruction can be estimated as Equation 1 (see

97   Equation 15 in Hausmann and Platt, 1994, Equation 3 in Le Bras and Platt, 1995, and Equation 7

98   in Zeng et al., 2006), or as Equation 2 if chlorine chemistry is considered through Reaction R9

99   (Equation IX in Platt and Janssen, 1995).

100      $-\frac{d[O_3]}{dt} = 2 \cdot k_3 \cdot [BrO]^2$ (1)

101      $-\frac{d[O_3]}{dt} = 2(k_3 \cdot [BrO]^2 + k_9 \cdot [BrO] \cdot [ClO])$ (2)

102   BrO + ClO → Br + OClO   (R9)
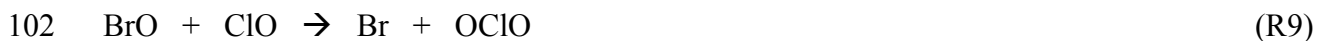
103   However, these approximations assume that the ozone destruction rate is dominated by the BrO

104   + XO reaction, which in turn necessitates efficient gas-phase recycling of Br; therefore, a

105   relatively long bromine chain length would be required to account for observed rates of ozone

106   destruction. It is, however, possible that Br atoms are generated mostly by Br_2 photolysis,

107   followed by BrO termination, e.g. by R5, in which case a short gas-phase bromine radical chain

108   length would be implied. The chain length for any process depends on the rates of the

109   propagation relative to the production and destruction reactions (Kuo, 1986). It is important to

110   note that the chain length refers to radical propagation reactions occurring solely in the gas phase,

111   and is a quantity completely independent of any condensed phase chemistry. In the stratosphere,

112   the Br/BrO catalytic cycle can have a chain length ranging from 10^2 to 10^4 (Lary, 1996). In the

113   troposphere, there is significantly less solar radiation and many more available sinks; thus,

114   radical chain lengths can be much shorter. For example, the chain length of the tropospheric

115   HO_x cycle has been estimated to be ~ 4 – 5 (Ehhalt, 1999; Monks, 2005), increasing to 10 – 20

116   near the tropopause (Wennberg et al., 1998). The halogen radical chain lengths in the Arctic

117   troposphere have so far not been determined, thus, it is difficult to evaluate whether Equations I

118   and II are appropriate for estimating ozone depletion rates.

119   The importance of heterogeneous reactions for recycling reactive bromine has been

120   demonstrated in the recent literature (see review by Abbatt et al., 2012). Modeling studies using

121   typical Arctic springtime conditions to simulate ODEs have concluded that ozone depletion

122   cannot be sustained without considering the heterogeneous recycling of reactive bromine on

123   snow or aerosol surfaces (e.g., Michalowski et al., 2000; Piot and Von Glasow, 2008; Liao et al.,

124   2012; Toyota et al., 2014). Michalowski et al. (2000) determined that the rate of ozone depletion

125   in their model was limited by the mass transfer rate of HOBr to the snowpack (effectively, the

126   rate at which Br is recycled through the heterogeneous mechanism) and that the depletion of

127   ozone is nearly completely shut down when snowpack interactions are removed. Piot and von

128   Glasow (2008) simulated ozone depletion using the one-dimensional MISTRA model and

129   concluded that major ODEs (defined as complete destruction within 4 days) could only be

130   produced if recycling of deposited bromine on snow is included. Without heterogeneous

131   recycling on the snowpack, the BrO_x termination steps and irreversible loss of HOBr and HBr to

132   the surface prohibits the occurrence of an ODE. More recently, using HOBr observations from

133   Barrow during OASIS, Liao et al. (2012b) found that a simple photochemical model over-

134   predicted observed HOBr during higher wind events ($> 6 \text{ m s}^{-1}$), ostensibly due to an under-

135   predicted heterogeneous loss to aerosol in the model, and concluded that their field observations

136   support the hypothesis of efficient recycling back to reactive bromine via this mechanism.

137   While it is evident that the reactions occurring on snow and aerosol surfaces are likely the

138   initial source of halogen species to the polar boundary layer and that heterogeneous bromine

139   recycling on these surfaces must be considered for HOBr and HBr (as well as $BrNO_2$ and

140    $BrONO_2$ in higher NO_x environments), the relative importance of gas-phase recycling of

141   bromine atoms is uncertain, as demonstrated by the use of gas-phase radical reaction rates to

142   estimate the ozone depletion rate. The goal of this work was to investigate gas-phase Br atom

143   propagation in terms of the bromine chain length in comparison to the production of Br atoms

144   through photolysis of Br_2 and BrCl, which are predominantly produced directly from surface

145   emissions. Here, we present results from our study using a zero-dimensional model constrained

146   with time-varying measurements of molecular halogens, HOBr, O_3, CO, NO, NO_2, and VOCs

147   from the 2009 Ocean-Atmosphere-Sea Ice-Snowpack (OASIS) campaign in Barrow, Alaska.

148   This work builds on the analysis presented in Thompson et al. (2015) using the same model

149 framework. By constraining our model with observations, we were able to conduct an in-depth

150 study of the halogen atom recycling occurring under varying conditions that were observed

151 during the campaign.

152

153 **2   Experimental**

154 **2.1 Measurements and Site Description**

155   The analysis presented herein utilizes observations conducted during the OASIS field

156 campaign that occurred during the months of February through April of 2009 in Barrow, AK.

157 The goal of the OASIS study was to investigate the chemical and physical processes occurring

158 within the surface boundary layer during ozone and mercury depletion events in polar spring.

159 This study resulted in the largest suite of simultaneous and co-located atmospheric measurements

160 conducted in the Arctic near-surface atmosphere to date, and represents a unique opportunity for

161 in-depth examination of a multitude of chemical interactions in this environment.

162   Atmospheric measurements were conducted from instrument trailers located near the

163 Barrow Arctic Research Consortium (BARC) facility on the Naval Arctic Research Laboratory

164 (NARL) campus. Winds arriving at the site are primarily northeasterly, from over the sea ice,

165 and thus represent background conditions with influence from natural processes and snow-air

166 interactions. Winds occasionally shift to westerly, bringing local emissions from the town of

167 Barrow to the site, however these isolated events are easily identifiable by coincident

168 enhancements in both NO_x and CO.

169   Measurements of molecular halogens, HOBr, NO, NO_2, O_3, CO, and VOCs were used to

170 constrain the model employed in this analysis. Instrumental methods for these measurements

7

171 have all been described elsewhere, thus, only a brief description is provided here. Inorganic

172 halogen species (Br_2, Cl_2, BrO, and HOBr) were measured by chemical ionization mass

173 spectrometry with I^- ion chemistry as described in Liao et al. (2011, 2012, 2014); O_3, NO, and

174 NO_2 were measured by chemiluminscence (Ridley et al., 1992; Ryerson et al., 2000). CO was

175 measured using a standard commercial CO analyzer (Thermo Scientific) with infrared absorption

176 detection, and formaldehyde (HCHO) was measured at 1 Hz frequency using a tunable diode

177 laser absorption spectrometer, as described in Fried et al. (1997) and Lancaster et al. (2000). A

178 large suite of organic compounds was measured in situ by fast GC-MS (Apel et al. 2010) and via

179 whole air canister samples with offline GC-MS (Russo et al., 2010).

180

181 **2.2 Model Description**

182 The model used for this study is a zero-dimensional box model developed using the

183 commercial software FACSIMILE. A detailed description of the model can be found in

184 Thompson et al. (2015). We will describe the model only briefly here.

185 Our model consists of 220 gas-phase reactions and 42 photolysis reactions, representing

186 much of the known gas-phase chemistry occurring in the Arctic, including the important halogen,

187 HO_x, NO_x and VOC chemistry associated with ozone depletions. The model also includes an

188 inorganic iodine reaction scheme adapted from McFiggans et al. (2000, 2002), Calvert and

189 Lindberg (2004) and Saiz-Lopez et al. (2008). Although IO has not been unambiguously

190 measured in the High Arctic above the $\sim 1.5 - 2$ pptv detection limit of LP-DOAS (long-path

191 differential optical absorption spectroscopy), observed enhancements in filterable iodide and

192 total iodine suggest that iodine chemistry is active to some extent in this region (Sturges and

193 Barrie, 1988; Martinez et al., 1999; Mahajan et al., 2010; Hönninger, 2002). Recently, I_2 has

194 been detected at tens of pptv within the snowpack interstitial air near Barrow, AK and at ≤0.5

195 pptv in the near surface air by I⁻ CIMS, providing direct evidence supporting the presence of at

196 least low levels of iodine chemistry (Raso et al., 2016). In our previous study (Thompson et al.,

197 2015), we investigated the impact of two different hypothetical levels of iodine. Here, we

198 investigate only the "Low Iodine" scenario for certain calculations, in which a diurnally varying

199 I_2 flux is incorporated such that average daytime mole ratios of IO remain near 1 pptv for the

200 majority of the simulation. These levels of IO are realistic given our current knowledge based on

201 the work of Hönninger (2002) and Raso et al. (2016).

202   All gas-phase rate constants used in this model were calculated for a temperature of 248

203 K, consistent with average daytime conditions in Barrow for the period simulated. Although

204 some gas-phase reactions can exhibit a significant temperature dependence, we chose not to

205 incorporate variable temperatures into our model. This is justified in this case because ambient

206 temperature in Barrow for the week of 25 March 2009 varied by less than 10 K between the

207 maximum and minimum recorded daily temperatures. The radical oxidation and radical-radical

208 reactions that are of primary importance here do not have a large temperature dependence

209 (Atkinson et al., 2006, 2007); for example, a variability of 10 K imposes an ~1% change on the

210 rate of ethane oxidation by Cl atoms and a <4% change on the rate of the BrO + BrO radical self-

211 reaction. Most radical-radical reactions have only a small negative-temperature dependence.

212 Furthermore, and as mentioned previously, the major non-radical chemical species driving the

213 model are highly constrained to observations and are not allowed to freely evolve. Table 1

214 contains an abbreviated list of the reactions included in the model, showing only those reactions

215 that are central to the production, propagation, and termination of bromine radical chemistry that

216 is the focus of this study. A complete list of reactions can be found in Thompson et al. (2015).

217   The model is configured to simulate 7 days during late March, 25 through 31 March, that

218   include a period of depleting ozone, a full ozone depletion ($[O_3] < 2$ ppbv) lasting $\sim$ 3 days, and

219   recovery. The O_3 time-series for this period is shown in Figure 1A, along with radiation as a

220   reference (all plots are in Alaska Standard Time).   We constrain the model to observations for

221   this time period by reading in time-varying data sets of O_3, C_2H_2, C_2H_4, C_2H_6, C_3H_8, C_3H_6, *n*-

222   C_4H_{10}, *i*-C_4H_{10}, HCHO, CH_3CHO, CH_3COCH_3, methyl ethyl ketone (MEK), Cl_2, Br_2, HOBr, NO,

223   NO_2, and CO at ten-minute time steps. All other gas-phase species are allowed to freely evolve.

224   Surface fluxes (represented as volumetric fluxes) are used for HONO and I_2 and are scaled to

225    $J(NO_2)$ as a proxy for radiation as both of these species are likely to be produced

226   photochemically. Further discussion regarding HONO can be found in Thompson et al. (2015).

227   Photolysis rate constants (*J* coefficients) for many of the species included were calculated

228   during OASIS using the Tropospheric Ultraviolent and Visible Radiation model from

229   measurements of down-welling actinic flux conducted throughout the campaign (Shetter and

230   Müller, 1999; Stephens et al., 2012). Estimates of J_{max} in the Arctic for OClO were taken from

231   Pöhler et al. (2010), for HOCl from Lehrer et al. (2004), and for $CHBr_3$ from Papanastasiou et al.

232   (2014). J_{max} values for the iodine compounds were calculated according the work of Calvert and

233   Lindberg (2004), which also simulated conditions for late March in Barrow, Alaska. Time-

234   varying *J* coefficients for O_3 and NO_2 were read into the model at 10-minute time steps. All other

235   photolysis reactions were scaled to $J(NO_2)$ in the modeling code using the maximum *J*

236   coefficients (J_{max}) for 25 March (a clear-sky day) as a scaling factor. For cloudy days, this

237   method assumes that *J* coefficients for other photolytically-active species are attenuated in a

238   manner that is proportional to $J(NO_2)$.

239   In the initial development of the model, heterogeneous reactions of halogen species

240   occurring on aerosol and snowpack surfaces were included, as well as mass transfer and dry

241   deposition for certain species using the method and mechanism of Michalowksi et al. (2000).

242   This mechanism assumes aqueous phase kinetics for those reactions occurring within a

243   uniformly distributed quasi-liquid layer (QLL), in a similar fashion as numerous other models

244   (e.g., Piot and von Glasow, 2008; Thomas et al, 2011; Toyota et al., 2014). It was originally

245   intended to utilize this multiphase chemistry to produce halogen radical precursors. However,

246   the heterogeneous production mechanisms could not reproduce observed Br_2 or Cl_2 from OASIS.

247   This reflects the complex but not fully understood condensed phase chemistry and physics that

248   leads to production of Br_2 (and Cl_2) (Abbatt et al., 2012; Domine et al., 2013; Pratt et al., 2013).

249   Additionally, the current knowledge of the physical properties of the QLL and the location of

250   liquid-like surfaces on snow grains would seem to invalidate the aforementioned assumptions on

251   which many of the current heterogeneous models are based (Domine et al., 2013), specifically

252   that the chemistry occurs in a liqui-like environment on snow grains. Indeed, Cao et al. (2014),

253   adopted a simplified heterogeneous chemistry mechanism in their modeling of Arctic ozone

254   depletion, wherein they use the mass transfer of HOBr to the surface as the rate-limiting step in

255   Br_2 production, citing the lack of suitable reaction mechanisms with which to properly simulate

256   condensed phase chemistry on snow/ice. Admittedly, our model is also not able to capture these

257   complex heterogeneous processes. However, as discussed thoroughly by Domine et al. (2013),

258   even our most complex state-of-the-art snow chemistry models are neither physically nor

259   chemically accurate, and rely upon a variety of adjustable parameters to produce reasonable

260   results, because of the lack of fundamental understanding of the actual phase and physical and

261 chemical environment in which the chemistry is occurring. It is thus clear to state that the

262 kinetics of the individual reactions in such a case cannot be reliably simulated.

263   In light of the limitations of all models of cryosphere photochemistry, a strength of this

264 study, and opportunity, rests with the fact that we have observations of key halogen species,

265 including Br_2, Cl_2, BrO, ClO, HOBr, as well as VOCs, NO_x, OH and HO_2. Therefore, to study

266 the gas phase recycling discussed in the Introduction, in this work Br_2 and Cl_2 concentrations

267 were fixed at the observed levels (see Thompson et al., 2015 for further discussion) and were not

268 produced via heterogeneous chemistry. During a period spanning a portion of 29 and 30 March,

269 Br_2 observations are not available due to instrument instability. Here, we have filled in the

270 missing portion of data with average daytime Br_2 values based on observations from 27 and 28

271 March and the morning data available for 29 March, and use average nighttime values for the

272 night of 29/30 March using the observations from the two adjacent nighttime periods. The filled-

273 in values for Br_2 result in reasonable agreement between modeled and observed BrO for this

274 period. In the analyses presented in Figures 3 and 5 – 10 we have indicated this period of missing

275 and filled-in Br_2 values with a shaded box. Due to the sparseness of BrCl observations during

276 OASIS, only daytime BrCl was used as produced in the model multiphase mechanism. While

277 we do not argue that the production mechanism for BrCl is accurate, the daytime simulated BrCl

278 mole ratios of 0 – 10 pptv are in approximate agreement with the available data for the campaign.

279 In any case, according to our model, BrCl was not a significant source of either Br or Cl atoms

280 relative to Br_2 and Cl_2.

281   Though we do not use the heterogeneous chemistry module for any chemical production

282 (other than BrCl), deposition and mass transfer is a significant and critical sink for certain

283 species. Thus, we do make use of this aspect of the multiphase portion of the model, as described

284 below. The dry deposition velocity of O_3 to the snowpack is estimated at 0.05 cm·s^{-1}, consistent

285 with previous measurements and modeling studies (Gong et al., 1997; Michalowski et al., 2000;

286 Helmig et al., 2007; Cavender et al., 2008), though it is recognized that there is large uncertainty

287 with this parameter from field observations (Helmig et al., 2007, 2012). Assuming a boundary

288 layer height of 300 m, this corresponds to a transfer coefficient, k_t, of 1.67x10^{-6} s^{-1}. Dry

289 deposition velocities for the stable Arctic environment have not been determined for the halogen

290 acids (HBr, HCl, HOBr, HOCl, HOI), therefore we use the estimation method of Michalowski et

291 al. (2000) and assume a deposition velocity that is 10 times greater than for O_3, leading to a k_t of

292 1.67x10^{-5} s^{-1}. We assume an equivalent k_t for the oxidized nitrogen compounds (HNO$_3$, HO$_2$NO$_2$,

293 HONO, N$_2$O$_5$, BrNO$_2$, and BrONO$_2$). The mass transfer coefficient of atmospheric species to the

294 particle phase is calculated as a first-order process as described in Jacob (2000). The

295 concentration of aerosol surface area used was 3.95 x 10^{-7} cm^2 cm^{-3} as calculated by

296 Michalowski et al. (2000) from measurements made at Alert by Staebler et al. (1994), with a

297 maximum aerosol radius of r = 0.1 μm. These levels are also consistent with observations of

298 aerosol surface area at Barrow, which ranged between 9 x 10^{-8} cm^2 cm^{-3} and 40 x 10^{-7} cm^2 cm^{-3}

299 (Liao et al. 2012b). We recognize, however, that this constant level of aerosols imparts a

300 constant loss rate in the model and does not take into account any variability in the deposition

301 strength. Because many of these species are lacking empirically-derived deposition velocities

302 (e.g, HOBr), there is necessarily large uncertainty in these values, and it is not possible at this

303 time to ascertain whether the uncertainty associated with the deposition velocity estimation is

304 greater or less than the uncertainty imposed by using a constant aerosol surface area. Liao et al.

305 (2012b) did use time-varying aerosol surface area from observations at Barrow, however, they

306 suggested that simple parameterization of deposition of HOBr to aerosols was insufficient for

accurately simulating HOBr (further discussion of HOBr is in Section 3.1). Given the highly

simplified nature of the surface deposition in our model, we do not attempt to differentiate

between deposition to aerosols and snow, and instead we lump these two terms together under

the "surface deposition" umbrella. However, while we mostly constrain the model to observed

HOBr, the comparison to simulated HOBr using these values is instructive.

3   Results and Discussion

3.1   Comparison of modeled and observed Br_2, BrO, HOBr, and HO_2

This work focuses on the propagation and production mechanisms of Br atoms, and thus

it is critical that our model accurately simulates BrO and Br_2 at mixing ratios that are consistent

with observations. Figures 1B and 1C show comparisons between simulated mixing ratios

(black trace) of Br_2 and BrO compared to the measured values during this time (red data) by

chemical ionization mass spectrometry (CIMS) (Liao et al., 2012b). Modeled BrO is presented

as hourly averages. In the model, Br_2 is fixed to time-varying observations, whereas BrO is

produced strictly through the gas-phase photochemical reactions. The model captures the overall

temporal profile and magnitude of BrO throughout the period. It should be noted, however, that

the uncertainty in the BrO measurements is large during ODEs as the observed values are very

near the detection limit (LOD of ~2 pptv with uncertainty of -3/+1 pptv near the LOD).

Br_2 mixing ratios reach 2 − 12 pptv (Figure 1B) during the daytime. Given the short

lifetime of Br_2 resulting from rapid photolysis, these daytime mixing ratios imply a large surface

flux, that in turn produces the BrO mole ratios observed. These Br_2 levels are consistent with

previous Arctic measurements that observed daytime Br_2 up to 27 pptv (Foster et al., 2001) and

agree well with the "uncorrected" Br_2 data reported in Liao et al. (2012a, 2012b) for this period.

330 It has been suggested that daytime Br_2 greater than the CIMS instrumental detection limit (~1

331 pptv) is an artifact of HOBr conversion to Br_2 on the instrument inlet using an aircraft inlet

332 (Neuman et al., 2010), however, for the instrument configuration employed during OASIS, it is

333 not clear how much, if any, of the Br_2 signal is a result of HOBr reactions on instrument surfaces.

334   An estimate of the effective mixing height of Br_2 can be calculated using the method of

335 Guimbaud et al. (2002) and using an average measured diffusivity during OASIS of 1500 cm^2 s^{-1}

336 (R. Staebler, personal communication, 2015). By assuming that photolysis is the dominant loss

337 mechanism controlling the Br_2 mid-day lifetime in a stable boundary layer typical of Arctic

338 conditions, the daytime effective mixing height is ~1.85 m. This also assumes that the snowpack

339 is the primary source of Br_2 emissions, which is consistent with previous assumptions for the

340 aldehydes (Sumner et al., 1999; Guimbaud et al., 2002) and is supported by direct empirical

341 evidence of the tundra snowpack being a relatively strong source of Br_2 (Pratt et al., 2013).

342 Enhanced Br_2 within the snowpack interstitial air has also been predicted from the modeling

343 studies of Toyota et al. (2011, 2014). From this estimation, the majority of the Br_2 present at the

344 surface would remain at the height of the instrument inlet (~1 m) in the sunlit periods. If

345 aerosols do represent a significant source of Br_2 as has been hypothesized, and inferred indirectly

346 from bromide depletion in sea salt aerosols (Sander et al., 2003), then one would expect

347 enhanced Br_2 to be present throughout the height of the boundary layer. In our highly constrained

348 model, daytime Br_2 mixing ratios greater than 1 pptv are necessary to reproduce observed BrO,

349 therefore, this modeling study suggests that Br_2 should indeed be present and above the

350 instrument detection limit during the daytime. Br atoms are predicted at concentrations ranging

351 from 1 x 10^7 to 3 x 10^9 molecules cm^{-3}. The hourly averaged model output for Br is shown in

352 Figure 2D. No direct measurements of Br atoms are available with which to compare, though

353   these values are within the range of estimates determined by Jobson et al. (1994) and Ariya et al.

354   (1998).

355   In the case of HOBr, our model originally simulated this species based on the known gas-

356   phase sources and sinks (including photolysis) and deposition/uptake to surfaces as described

357   above. As shown in Thompson et al. (2015), and again in Figure 2A, given the observed Br_2

358   mixing ratios, the model greatly overestimated HOBr. Liao et al. (2012b) also simulated

359   inorganic bromine species from the OASIS campaign using a simple steady-state model and

360   experienced that their model also overestimated the observed HOBr, with the overestimation

361   becoming especially pronounced during periods of higher winds. They suggested a faster

362   heterogeneous loss to aerosols or blowing snow that was not represented in their model, despite

363   utilizing time-varying aerosol surface area from observations. For the majority of the results

364   presented in this work, we chose to operate our model constrained to HOBr observations, as

365   illustrated in Figure 2B. Figure 2C shows modeled HOBr obtained by adjusting the deposition to

366   aerosols based on daily wind speeds, and tuned to provide reasonable agreement with

367   observations. This resulted in smaller deposition rates on 25 through 27 March when winds were

368   calm, and higher deposition rates on 29 through 31 March when winds were up to 9 m/s. This

369   method allowed us to calculate the importance of surface deposition of HOBr relative to

370   photolysis as a sink for this compound, but the constrained version of the model was used for all

371   other calculations, e.g. for the chain length calculations.

372   HO_2 is essential for the heterogeneous recycling of bromine (via Reactions R5 – R7).

373   Therefore, it is important that our model provides a reasonable estimation of HO_2 for this

374   analysis. In Figure 1E we show a comparison of simulated, hourly-averaged HO_2 (black trace)

375   and observed HO_2 from OASIS for this period (red data), measured using a CIMS developed for

16

376   peroxy radicals (Edwards et al., 2003). Our model captures the diurnal cycle of HO_2 and the

377   daily fluctuations observed. Simulated HO_2 is on the lower limit of observations for 25 and 29

378   March, and does not reach the maximum mixing ratios observed. The model also somewhat

379   overpredicts HO_2 on 28 through 30 March, however, the model values are within the stated 25%

380   - 100% range of uncertainty of the measurement.

381

382   **3.2 Chain length**

383   The ozone destruction cycle as described in Reactions R1 − R3 is a chain reaction

384   mechanism catalyzed by BrO_x. The effectiveness of a catalytic cycle can be can be quantified by

385   considering the chain length, that is, the number of free radical propagation cycles per

386   termination or per initiation. The radical chain length is a metric that refers solely to gas phase

387   reactions (Monks, 2005). We have not, until the OASIS2009 campaign, had the high quality

388   measurements available to enable a reliable estimation of the bromine radical chain length in the

389   Arctic.

390   The length of the chain in a radical propagation cycle is limited by termination steps that

391   destroy the chain carriers and result in relatively stable atmospheric species. Thus, the chain

392   length can be defined as the rate of propagation divided by the rate of termination. Alternatively,

393   the chain length can also be calculated using the rate of initiation. If the total bromine radical

394   population is at steady-state, the rate of initiation is equal to the rate of termination; thus, for

395   short-lived radical species, the two methods for calculating chain length should be approximately

396   equal.

397   Method 1: $\Phi = \dfrac{\Sigma(\text{Rates of propagation})}{\Sigma(\text{Rates of termination})}$ (3)

398   Method 2: $\Phi = \dfrac{\Sigma(\text{Rates of propagation})}{\Sigma(\text{Rates of initiation})}$ (4)

399   We used our model to calculate the chain length for bromine radical propagation across

400   the 7-days of the simulated period using both Method 1 and 2 as shown in Equations 5 and 6.

401   Because bromine radicals are generated photolytically, the chain length is calculated for daytime

402   only, defined here as approximately 7:00 to 20:00 Alaska Standard Time (AKST).

403

404   Method 1:

$$\Phi_{Br} = \frac{(2k[BrO]^2 + J_{BrO}[BrO] + k[BrO][ClO] + k[BrO][IO] + k[BrO][CH_3OO] + k[BrO][OH] + k[BrO][O(^3P)] + k[BrO][CH_3COOO] + k[BrO][NO])}{(k[Br][HO_2] + k[Br][C_2H_2] + k[Br][C_2H_4] + k[Br][C_3H_6] + k[Br][HCHO] + k[Br][NO_2] + k[Br][CH_3CHO] + k[Br][C_3H_6O] + k[Br][C_4H_8O] + k[Br][CH_3OOH] + k[BrO][HO_2] + k[BrO][CH_3OO] + k[BrO][C_3H_6O] + k[BrO][NO_2])} \quad (5)$$

405
406
407
408
409
410
411
412
413
414
415
416

417   Method 2:

$$\Phi_{Br} = \frac{(2k[BrO]^2 + J_{BrO}[BrO] + k[BrO][ClO] + k[BrO][IO] + k[BrO][CH_3OO] + k[BrO][OH] + k[BrO][O(^3P)] + k[BrO][CH_3COOO] + k[BrO][NO])}{(2J_{Br2}[Br_2] + J_{BrCl}[BrCl] + J_{HOBr}[HOBr] + J_{BrONO2}[BrONO_2] + J_{IBr}[IBr] + J_{BrNO2}[BrNO_2] + J_{CHBR3}[CHBr_3] + k[HBr][OH] + k[CH_3Br][OH] + k[CHBr_3][OH])} \quad (6)$$

418
419
420
421
422
423
424

425 Termination reactions for bromine include those reactions that are sinks for either Br and BrO,

426 since Br and BrO rapidly interconvert. Here, photolysis of BrO and the BrO + NO reaction is

427 included in the numerator because they are efficient at reforming Br and propagating the chain;

428 however, these reactions do not result in a net loss of ozone. Photolysis of BrO produces atomic

429 oxygen that reacts with O_2 to form O_3, and NO_2 can photolyze to similarly reform O_3. Therefore,

430 it should be noted that if we omit these reactions and consider only those that result in a net O_3

431 loss, it would be expected that the chain length would be shorter. Indeed, model simulations were

432   performed without these two terms and the determined chain lengths were on average 80% lower

433   than those presented here. BrO reaction with CH_3OO is included in both the numerator and

434   denominator in Equation 5 because this reaction has two channels, one that propagates the Br

435   chain and one that terminates it.

436   In Figure 3, we present the hourly-averaged results of these calculations for the Base

437   Model, which show that the two methods for calculating bromine chain length are in reasonably

438   good agreement, although there are small differences between the two methods throughout the

439   time-series. This agreement is a test of our basic understanding of the radical chemistry. The

440   inset graph in Figure 3 shows a linear regression of the two methods for the chain length

441   calculation. The coefficient of determination (r^2) of 0.93 confirms the good temporal agreement

442   between the two methods. However, the slope of 0.68 indicates that Method 1 is generally higher

443   than Method 2 throughout (with some periods of exception). This offset reveals that either

444   Method 1 is slightly overestimating the chain length, or that Method 2 is underestimating it. The

445   numerator is identical in Equations 5 and 6, therefore, the denominator must be driving this

446   discrepancy, with either the denominator term in Method 1 too low or the denominator term in

447   Method 2 too high (or some combination thereof). If it's the case that the Method 1 denominator

448   is too low, then it must be concluded that there are important BrO_x terminations that are missing

449   from the calculation. If, however, the denominator of Method 2 is too high, this would imply that

450   our measurements of these BrO_x precursors are too high, which, as discussed above, is a known

451   possibility at least for the Br_2 measurements. The photolysis of Br_2 is the dominant initiation

452   pathway (see Section 3.3), therefore, the Method 2 chain length calculation would be the most

453   sensitive to Br_2 measurement inaccuracies.

454   In Equation 6, we included photolysis of the most prevalent organobromine compound

455   bromoform for completeness, though it has been recognized for many years that the rate of Br

456   atom production from this pathway is small (e.g., ~ 100 molecules·cm^{-3}·s^{-1} for bromoform at

457   mid-day) compared to Br atom production from Br$_2$ photolysis (~1.3x10^7 molecules·cm^{-3}·s^{-1} at

458   mid-day assuming 5 pptv of Br$_2$). Photolysis of bromine nitrate (BrONO$_2$) and nitryl bromide

459   (BrNO$_2$) are also included, however, the prevalence of and production of these compounds in the

460   Arctic is highly uncertain, and no observations of these species in the Arctic have been published

461   to date with which to compare to our modeled mixing ratios. Inclusion of these terms at the

462   modeled BrONO$_2$ and BrNO$_2$ mixing ratios has a small effect on the calculated chain length that

463   cannot account for the discrepancy between the two methods.

464   The median bromine chain-length in the Base simulation, averaging the results from

465   Method 1 and Method 2, is ~1.2 across daylight hours (7:00 to 21:00 AKST) and ~2 for mid-day,

466   defined for this purpose as approximately 12:00 until 18:00 AKST, when [O$_3$] ≥ 5 ppbv. In

467   comparison, the bromine chain length is ~0.4 when [O$_3$] < 5 ppbv (Figure 3). In other words, the

468   chain cannot be maintained when [O$_3$] < 5 ppbv. Under these conditions, Br atoms readily

469   terminate, e.g. via reaction with CH$_3$CHO (see below). 29 March exhibits an early morning

470   enhancement in the chain length. This morning spike appears to correlate with a similar sharp

471   increase in ozone. Br$_2$ accumulates during the nighttime hours, resulting in the highest Br$_2$

472   concentrations in the early morning hours (Figure 1B). When the sun rises, Br$_2$ photolyzes

473   rapidly, releasing a pulse of reactive bromine that converts to BrO in the presence of ozone. This,

474   in concert with the coincident increase in ozone, can explain the enhanced chain length during

475   the early morning hours.

476　　　　Overall, midday bromine chain lengths remain near or below 2 during background O_3

477　　days.　This implies that, for these days, ozone depletion is strongly dependent upon initiation

478　　processes, and most BrO radicals produced terminate the chain via reactions R5 and R10 (below)

479　　in less than two cycles. Reaction R12 (below) will also efficiently terminate the chain, however,

480　　the relative importance of R10 and R12 depend upon the relative abundances of BrO and Br. For

481　　background O_3 days, such as 29 and 30 March, [BrO] > [Br], thus, R10 > R12.　The low chain

482　　lengths calculated here are surprising, given that it has been generally accepted that Br is

483　　recycled efficiently in the gas-phase.　That it appears this is not the case supports the conclusions

484　　of Michalowski et al. (2000), Piot and von Glasow (2008), and Toyota et al. (2014) that

485　　heterogeneous recycling through the "bromine explosion", which emits Br_2 and BrCl from

486　　surface reactions, is of critical importance to sustain ODEs occurring at the surface.

487　　　　A question to address regarding the relatively small chain length calculated for Br is to

488　　what extent the chain length is dependent on NO_2.　As discussed in Thompson et al. (2015) and

489　　further investigated in Custard et al. (2015), NO_2 at Barrow can be greater and more variable

490　　than at very remote sites due to its proximity to anthropogenic emissions sources.　We find that

491　　the chain length calculation is relatively insensitive to NO_2 concentrations and so it is robust for

492　　the range of conditions encountered at Barrow.　This is shown in detail in Custard et al. (2015).

493　　As discussed by Custard and coworkers, while NO_2 can inhibit the bromine chain through

494　　reactions R10 and R12 (i.e., decreasing the chain length), enhanced NO_2 will also reduce

495　　available HO_2, thereby decreasing the HO_2 available to terminate the chain (i.e., increasing the

496　　chain length). While the Method 2 calculation does not contain NO_2 in the denominator, the

497　　absolute [BrO] is NO_x-dependent because of reaction R10 (Custard et al., 2015), and it is through

498　　this effect that high NO_x mixing ratios act to decrease the rate of O_3 depletion.　In the natural

499 environment, Br_2 production can potentially also be NO_x-dependent, e.g. via reaction R11,

500 followed by R7. While our model does not *simulate* the condensed phase processes, it is

501 sensitive to them, since the model is constrained to the product of those processes, Br_2.

502          $BrO + NO_2 \rightarrow BrONO_2$ (R10)

503          $BrONO_{2(aq)} + H_2O \rightarrow HOBr + HNO_3$ (R11)

504          $Br + NO_2 \rightarrow BrNO_2$ (R12)

505 However, for the period of 26 through 30 March, NO_x was relatively low, and the relatively good

506 agreement between the two calculation methods further supports our conclusion.

507   To investigate how chemical interactions with chlorine and iodine affect the bromine

508 chain length, a series of simulations was performed by varying the combinations of halogens

509 present in the model. The bromine chain length was determined for scenarios with only Br, Br

510 and Cl (Base Model), Br and Iodine, and Base with Iodine. Simulations without chlorine were

511 performed simply by removing Cl_2, while simulations with iodine were performed by

512 incorporating the I_2 flux as described in Section 2.2. No other adjustments were made to the

513 model for these sensitivity runs.

514   Table 2 shows the results for both chain length calculation methods (i.e., Equations 5 and

515 6) for the different halogen combinations for the three days when ozone was present near

516 background values: 25, 29 and 30 March. For the Base scenario ("Br and Cl"), the average of the

517 median daily values for the bromine chain length is 1.43 and 1.05 for Method 1 and Method 2,

518 respectively. In comparison with the "Br Only" run, Cl chemistry does not induce a net increase

519 in the Br chain length, but rather causes a slight decrease. Cl chemistry can increase Br radical

520 propagation through the addition of the BrO + ClO cross-reaction and enhancement of the BrO +

521 CH_3OO radical propagation terms. However, Cl chemistry can also increase the concentration of

522 reactive bromine sinks, such as aldehydes (e.g., propanal and butanal, which were free to evolve

523 in our model; HCHO and CH_3CHO are fixed to observations) and HO_2 (see Thompson et al.,

524 2015). Iodine has the effect of increasing the Br chain length. When low levels of iodine are

525 added to the "Br Only" simulation, the chain increases from 1.52 to 1.59 in the Method 1

526 calculation, primarily due to the very fast cross-reaction between IO and BrO. The addition of

527 Cl to the "Br and I" simulation imparts a slight decrease to the Br chain length. This may be

528 explained by the competition between BrO and ClO for reaction with NO and/or IO, as well as

529 the additional Br sinks in the presence of Cl chemistry. Regardless, overall there is more Br

530 available for reaction with O_3 when Cl is present due to the interhalogen reactions, thereby

531 increasing the rate of ozone depletion (see Thompson et al., 2015 for further discussion on ozone

532 depletion rates).

533   There are several conclusions that can be drawn from Figure 3 and Table 2: 1) there is a

534 distinct difference in bromine chain length between O_3-depleted and non-depleted days with a

535 significantly larger chain length when ozone is present, and 2) for all simulations, the average

536 bromine chain is much shorter than expected (given that gas-phase recycling has, to date, been

537 assumed to be highly efficient). The chain length is greatest when ozone is present because

538 many of the species that propagate the Br chain (e.g., BrO, ClO, IO, and to a lesser extent OH

539 and CH_3OO) require O_3 for production. Although the relationship between bromine chain length

540 and BrO is not straightforward due to the multitude of interactions between BrO and other

541 species that either propagate or terminate the chain, the chain length does exhibit a rough

542 dependence on [BrO], shown in Figure 4, that can be loosely described with a linear fit. If it

543 were the case that the gas-phase Br chain length was relatively long (such that the numerator far

544 outweighs the denominator), and dominated by the BrO self-reaction, the numerator in Equations

545   5 and 6 would reduce to $2k[\text{BrO}]^2$, and the regression in Figure 4 would display a quadratic fit;

546   however, that is not observed here.

547   For purposes of comparison, the chain lengths for Cl and I were also calculated in a

548   manner analogous to that of Equation 5. These results are shown as hourly averages in Figure 5

549   for the Base with Iodine scenario. It is apparent from this figure that reactive chlorine exhibits

550   an exceptionally short chain length, whereas reactive iodine has a relatively long chain length.

551   The average Cl chain length across the three days of background ozone (25, 29, and 30 March) is

552   0.15, or 0.23 considering only mid-day hours (12:00 − 18:00 AKST). This result indicates that

553   nearly all Cl atoms that are produced terminate, likely through the very efficient reaction with a

554   multitude of VOCs, as shown in Thompson et al. (2015). This behavior also helps explain why

555   Cl has only a small effect on the bromine chain length. In contrast, I and IO have few known

556   sinks, which results in a reactive iodine chain length of 5.7 on average over 25, 29, and 30 March,

557   and 7.3 over only mid-day hours, with maxima over 12. The high efficiency of the gas-phase

558   regeneration of I in part explains why iodine is more efficient on a per atom basis at depleting

559   ozone than either Br or Cl (Thompson et al., 2015).

560

561   **3.3 Reactive bromine initiation, propagation, and termination pathways**

562   The individual reactions that initiate, propagate, and terminate the reactive bromine chain

563   were examined to determine the most important reaction pathways contributing the chain

564   reaction. The rates of Br atom production from the most important initiation pathways are

565   shown as hourly averages in Figure 6, with the y-axes expressed as the cumulative rate of

566   reaction, including all five precursors. These are reactions that produce Br atoms from stable

567   reservoir species, which is an important distinction from the propagation reactions that produce

568 Br atoms through radical reactions. Br_2 photolysis is calculated as 2 x $J_{Br2}[Br_2]$. Here, we do not

569 separate Br_2 produced in the gas-phase versus that directly emitted from a surface (this will be

570 discussed further in Section 3.5). The contribution of Br_2 photolysis in producing Br atoms vastly

571 dominates the cumulative production rate (Figure 6A). Therefore, in Figure 6B we show the

572 initiation terms without Br_2 photolysis so that these other production pathways can be visualized.

573   Effectively, Br_2 photolysis alone controls the production of bromine atoms, while the

574 remaining initiation pathways combined add only a minor contribution. Among the minor

575 pathways, HOBr photolysis is the most significant during non-ODE days, with the exception of

576 the high NO_x period of March 25, where $BrNO_2$ has the largest impact. In a highly polluted

577 environment, halogen cycling through NO_x reservoirs would become significantly more

578 important, as has been observed with $ClNO_2$ in mid-latitude regions (Thornton et al., 2010;

579 Mielke et al., 2011; Young et al., 2012). The small contribution of HOBr photolysis to bromine

580 atom production is an important point, because the gas-phase BrO + HOBr ozone depletion cycle

581 (that proceeds via HOBr photolysis rather than surface deposition) has been considered to be

582 significant previously (see, e.g., Hausmann and Platt, 1994), though Zeng et al. (2006) note that

583 HOBr photolysis has only a small effect on BrO_x cycling. Using the version of our model that is

584 unconstrained to HOBr, but incorporates a larger surface deposition in order to reproduce

585 observations (Figure 2C), we were able to determine that photolysis accounts for 19% of the

586 HOBr sink integrated over the 7-day simulation period. Surface deposition accounts for 80%,

587 and other known gas-phase reactions (HOBr + Br, HOBr + Cl, HOBr + OH, HOBr + O) are only

588 minor sink terms at a combined 1%. This corroborates the work of Zeng et al. (2006).

589   The cumulative rates of reaction of the most important propagation pathways, with and

590 without iodine, are shown in Figure 7 A and B. The rate of the BrO + BrO reaction is calculated

591   as $2k[BrO]^2$, since this reaction results in the production of two Br atoms. The reaction pathways

592   that dominate the bromine propagation, i.e., BrO photolysis and reaction with NO, are those that

593   do not result in a net ozone loss. This has been previously recognized and applied to Br steady-

594   state calculations in several works (e.g., Platt and Janssen, 1995; Zeng et al., 2006; Holmes et al.,

595   2010), and demonstrates that much of the time BrO regenerates Br without a net loss of ozone

596   for the simulated conditions in Barrow. Indeed, in our previous paper, we calculated that ~70%

597   of gas-phase BrO reforms ozone via photolysis or reaction with NO over this period (Thompson

598   et al., 2015). The inset pie charts, which show the average fractional importance of the various

599   propagation reactions for 29 and 30 March, reveal that these two pathways account for 84 – 91%

600   of the total.   Interestingly, the BrO self-reaction is small in comparison, with an average

601   contribution of 5 – 6%, and a maximum of 46%. However, if we consider only those reactions

602   that *do* lead to a net ozone loss, then the BrO self-reaction accounts for an average of 71% and a

603   maximum of 98% of the propagation. The rate of the BrO + ClO reaction rate is much smaller

604   than that for BrO + BrO, though not insignificant. While on average this reaction pathway

605   accounts for only 2%, it does reach 16% when Cl_2 is high on 29 March. In considering only

606   those reactions that result in a net ozone loss, the BrO + ClO pathway accounts for 21% on

607   average, and up to a maximum of 57%. In Panel B, the Base with Iodine scenario is shown. At

608   these levels, the BrO + IO reaction contributes 4%, which is at times comparable to BrO + BrO

609   and greater than BrO + ClO, even at the low IO mixing ratios in this simulation (~1 pptv).

610   The short gas-phase chain length calculated for bromine propagation indicates that there

611   are large reactive bromine (BrO_x) sinks terminating the chain reaction. Figure 8 presents the

612   rates of the most important BrO_x termination reactions, with the y-axis expressed as the

613   cumulative rate of reaction. Here it can be seen that reaction of BrO with NO_2 is the dominant

614 sink for BrO$_x$ on non-ODE days for the conditions encountered at Barrow, while Br reaction with

615 CH$_3$CHO is most important when O$_3$ is depleted. That HO$_2$ is a significant sink, and would be

616 more so in less anthropogenically-impacted Polar Regions, points toward the importance of

617 heterogeneous recycling through the bromine explosion mechanism. During ozone depletion,

618 such as the major event from days 26 − 28 March ([O$_3$] < 5ppbv) when BrO is mostly absent,

619 CH$_3$CHO becomes the primary sink term for Br, and HCHO is relatively more important. The

620 strength of the CH$_3$CHO sink is much greater than is HCHO, as noted previously by Shepson et

621 al. (1996) and Bottenheim et al. (1990). Of note are the relatively similar magnitudes for the

622 total rate of reaction of the initiation, propagation, and termination reactions shown in Figures 6,

623 7, and 8, respectively, which of course must be the case for a chain length near 1. This accounts

624 for the short bromine chain length determined here and also indicates that to sustain elevated

625 bromine radical concentrations necessary to deplete O$_3$ requires a relatively large Br$_2$ source,

626 likely in the form of a significant flux of Br$_2$ from the snow surface, or from in-situ production

627 from aerosols.

628

629 **3.4 Ozone loss rate**

630 Since the chain length calculations seem to suggest a larger than expected contribution of

631 heterogeneous bromine recycling to Br atom production, to examine this further, we calculated

632 the rate of net ozone loss by Br and Cl in the Base Model using Equation 7 and compared this

633 rate to that using the estimation method presented in previous works as shown in Equation 2

634 (Platt and Janssen, 1995; Le Bras and Platt, 1995). Additionally, the total simulated chemical

635 ozone loss in the Base Model was calculated from Equation 8, which includes O$_3$ destruction by

636 OH, HO$_2$, and photolysis (determined here as $k[O(^1D)][H_2O]$).

637 $O_3\ Loss\ by\ Br\ and\ Cl\ =\ (k[Br][O_3] - J[BrO] - k[BrO][NO])$ (7)
638 $+\ (k[Cl][O_3] - J[ClO] - k[ClO][NO])$

639 $Total\ Chemical\ O_3\ loss\ rate\ =\ k[Br][O_3] + k[Cl][O_3] + k[O(^1D)][H_2O]$ (8)
640 $+\ k[OH][O_3] + k[HO_2][O_3] - k[BrO][NO]$
641 $-\ J[BrO] - k[ClO][NO] - J[ClO]$

642 The method in Equation 2 assumes that the rate of ozone loss is equivalent to the rate at which

643 Br is regenerated through BrO reaction with itself and ClO (thus assuming efficient gas-phase

644 propagation and a long chain length), whereas Equation 7 accounts for all net ozone destruction

645 by Br and Cl, by correcting for those reactions that release a triplet oxygen atom and reform O_3.

646 In other words, this method accounts for the fact that some BrO radicals react to terminate the

647 chain (and at steady state, an equivalent BrO_x production rate is necessary). Figure 9A compares

648 these two estimations for O_3 loss rate in green (Equation 2) and pink (Equation 7). This

649 comparison clearly shows that there is a large difference between the methods, with the

650 estimation from Equation 2 significantly smaller overall. Additionally, the total chemical O_3 loss

651 (calculated by Equation 8) is shown in the dashed black trace. The O_3 loss rate estimation

652 presented in Equation 7 accounts for nearly all of the chemical O_3 loss (i.e., most chemical O_3

653 loss is a result of halogen chemistry), such that the dashed black line lies nearly perfectly on top

654 of the pink shaded regions.

655 In Figure 9B, we show a regression of the two estimation methods (Equation 2 in green

656 and Equation 7 in pink) versus the total chemical O_3 loss rate (Equation 8). Here it can be seen

657 from the pink data that halogen chemistry accounts for 99% of the total chemical O_3 loss under

658 the conditions simulated here. Importantly, the O_3 loss rate estimation presented in Equation 2

659 accounts for only 44% of the total chemical O_3 loss rate.

660   In the 1994 work by Hausmann and Platt, the authors also considered the BrO + HO gas-

661 phase ozone depletion cycle as a proxy for estimating the O_3 loss rate, using the equation shown

662 below (Equation 17 of Hausmann and Platt, 1994).

663       $-\frac{d[O_3]}{dt} = (k_5 \cdot [BrO] \cdot [HO_2])$ (9)

664 The authors only considered the gas-phase cycle of HOBr here with the photolysis of HOBr

665 regenerating Br. At the time of this publication, the heterogeneous cycling of HOBr had only

666 recently been proposed and had not been fully validated. Hausmann and Platt showed that

667 Equation 9 resulted in a significantly lower estimation for O_3 depletion than did Equation 1,

668 which considered only the BrO-BrO cycle. In Figure 9B, we show also the O_3 loss rate estimated

669 using Equation 9 in blue. Our results corroborate that of Hausmann and Platt (1994), and

670 demonstrate that Equation 9 can account for only 18% of the O_3 loss. This is also supported by

671 our results discussed previously that show that only 19% of HOBr is lost to photolysis. To

672 examine this one step further, we present an additional regression in Figure 8B (orange trace)

673 that combines Equations 2 and 9, thereby considering the three predominant gas-phase O_3

674 depletion cycles of BrO-BrO, BrO-ClO, and BrO-HO_2. This still can only account for 60% of the

675 O_3 loss.

676   Our analysis quantitatively expresses the conclusion that the gas-phase recycling of

677 bromine is not as efficient as previously considered and that it is often the case, for Barrow, that

678 BrO_x terminations must often, through reactions R5 or R10, be followed by heterogeneous

679 production of Br_2 through condensed-phase reactions of HOBr and/or $BrONO_2$. An important

680 conclusion from this analysis is that the chemical O_3 loss rate is largely underestimated when

681 calculated from only BrO observations using the previously accepted $2(k[BrO]^2 + [BrO][ClO])$

682 method, and one should be cautious about drawing conclusions about O_3 depletion rates and

29

683 timescales based solely on BrO observations. This may have significant impacts on the process

684 of examining ODEs and addressing the extent to which they represent local scale chemistry

685 versus transport effects. While this situation is significantly impacted by local NO_x sources at

686 Barrow, NO_x is expected to increase with development around the Arctic.

687

688 **3.5 Bromine atom production**

689   If it is the case that heterogeneous recycling is of such importance, it may be that

690 Reaction R5 (BrO + HO_2) competes favorably with Reaction R3 (BrO + BrO). Panel A of

691 Figure 10 shows the rates of reactions R5 and R3.   This plot demonstrates that for our modeling

692 results the rate of reaction of BrO with HO_2 is often of a comparable or greater magnitude than

693 the BrO self-reaction, and remains significant throughout the simulated period. Previous

694 modeling work by Sander et al. (1997) also compared the rates of these two critical reactions

695 (Figure 2 of that work). In contrast to our results, their model predicted that the rate of the BrO +

696 BrO reaction was up to a factor of 8 greater than that of BrO + HO_2. The reason for this

697 difference may perhaps be the much lower mixing ratios of HO_2 in the model by Sander and

698 coworkers. Their model predicted HO_2 daily maxima of 0.2 to 0.6 pptv for most days, increasing

699 to 1.8 pptv on the final three days of their simulation. In contrast, HO_2 observations at Barrow

700 were frequently greater than 5 pptv and up to 10 pptv. As demonstrated in Thompson et al.

701 (2015), HCHO was a dominant factor in controlling the HO_2 mixing ratios in Barrow. The low

702 levels of HO_2 in Sander et al. (1997) likely also contribute to their low predicted HOBr mixing

703 ratios, which do not exceed 1 pptv in their model. This also is much lower than observations at

704 Barrow, where HOBr reaching 10 pptv to 20 pptv was measured during our simulated period.

705 Because the BrO + HO_2 reaction is of primary importance for the bromine explosion mechanism,

706 our result supports the hypothesis that heterogeneous recycling may be equally or even more

707 important than gas-phase recycling of reactive bromine.

708   Given that the chain length is small, it must be that initiation is an important source of Br

709 atoms in order to sustain BrO and lead to O_3 depletion. To further examine the question of

710 surface emissions versus gas-phase recycling, we determined the rate of production of Br atoms

711 via photolysis of Br_2 and BrCl (Equation 10) compared to the rate of production of Br atoms

712 through gas-phase recycling calculated by Equation 11. Because our model is constrained by Br_2

713 observations and we do not produce Br_2 from surfaces via heterogeneous reactions, the

714 photolysis of Br_2 includes Br_2 that is both emitted from surfaces and that is formed via gas-phase

715 reactions. To correct for the Br_2 that is formed in the gas-phase reactions so that Equation 10

716 represents our best approximation for surface-emitted Br_2, we created a proxy in the model, Br_2^*,

717 that represents the Br_2 produced from gas phase reactions. These reactions include $Br + BrNO_2$,

718 $Br + BrONO_2$, and the BrO + BrO branch that produces Br_2. Equation 10 is thus corrected for the

719 gas-phase generated Br_2 by subtracting the photolysis of Br_2^*. A comparison of Br_2 and Br_2^*

720 reveals that these three gas-phase production pathways account for an average of 35% of

721 observed Br_2, suggesting that the snowpack and/or aerosols emits the remaining 65%. Again, we

722 cannot distinguish between snow or aerosol production using this method.

723

724 *Br Production from Surface-derived Br_2, BrCl* $= 2 \times J_{Br2}[Br_2] + J_{BrCl}[BrCl] - 2 \times J_{Br2}[Br_2^*]$ (10)
725
726
727 *Br Production via Gas-phase Recycling* $= 2k[BrO][BrO] + k[BrO][ClO]$ (11)
728                            $+ k[BrO][NO] + k[BrO][OH] + k[BrO][O(^3P)]$
729                            $+ k[BrO][CH_3OO] + k[BrO][CH_3COOO]$
730                            $+ J_{HOBr}[HOBr] + J_{BrO}[BrO] + J_{BrONO2}[BrONO_2]$
731                            $+ J_{BrNO2}[BrNO_2]$
732

733   Panel B of Figure 10 compares the results of Equations 10 and 11, showing the total rate of Br

734   atom production separated into Br production from the derived "surface-emitted" Br_2 and BrCl

735   (purple) and from gas-phase Br recycling (orange); Panel C plots the fraction of total Br atom

736   production that is due to production from Br_2 and BrCl surface emissions. The majority of the

737   time during this 7-day period Br atom production from Br_2 and BrCl emissions (Equation 10)

738   accounts for 30% or greater of the total, and at times reaches up to 90%. This explains both how

739   ozone depletion can be rapid despite the short calculated bromine radical chain length, as well as

740   the difference found between the two methods of estimating O_3 loss rate in Figure 9. It is

741   concluded from this analysis, then, that the condensed phase recycling of bromine can be of

742   equal or greater importance to the evolution of ODEs than gas-phase Br regeneration through

743   radical recycling reactions.

744

745   **4 Conclusions**

746   The analysis presented here suggests that the gas-phase recycling of bromine species may

747   be less important than commonly believed, and we conclude that heterogeneous recycling is

748   critical for the evolution of ODEs/AMDEs, consistent with results by Michalowski et al. (2000),

749   Piot and von Glasow (2008), and Toyota et al. (2011, 2014). To support this conclusion, we have

750   used the gas-phase bromine chain length, which has not previously been applied to Arctic

751   halogen chemistry, as an objective metric. The gas-phase bromine chain length is much shorter

752   than expected, suggesting that much of the Br present in the gas-phase is Br from surface

753   emissions. Again note that our calculation of chain length includes photolysis of BrO and BrO +

754   NO, which do not result in net O_3 loss. Had we omitted these two reactions, which we have

755   found are in fact dominating the radical propagation, the chain length would be, on average, 80%

756   shorter. Because of the small chain length calculated for Br, one must be cautious about drawing

conclusions about O_3 depletion from BrO measurements alone. We recommend concurrent measurements of a broad suite of inorganic bromine species for accurate study of these ozone depletion events. The very low mixing ratios of HOBr predicted by Sander et al. (1997) and the high mixing ratios originally predicted by our model point to the need for measurements of these species to validate the accuracy of Arctic models.

We find that between $30 - 90$% of Br atoms are produced from surface emissions of Br_2 and BrCl, though we cannot distinguish snow sources from aerosol sources using our model. However, it is important to note that we do not know how much of the condensed phase Br_2 production derives from reaction R7, or from some other condensed phase process, e.g. oxidation of Br^- by OH radicals (Abbatt et al., 2010). The in situ snow chamber experiments by Pratt et al. (2013) demonstrate a strong Br_2 source from the snowpack; similar field observations proving significant Br_2 emissions from Arctic aerosol are currently lacking. If the snow surface is the primary sources of these emissions, then a strong vertical gradient would be expected in the near surface boundary layer, and our estimations for the Br chain length would be only valid for the height of our measurements ($\sim$ 1 m above the snow). Strong deposition to the snow would also induce a vertical gradient in these species. If, however, aerosols are an important source of Br_2 (or other halogen precursors), then Br_2 production should occur throughout the entire height of the boundary with no significant vertical gradient, in a similar fashion as has been observed for $ClNO_2$, which is a known product of aerosol chemistry (Young et al., 2012). It is clear that vertically-resolved measurements of these halogen precursors are imperative for our understanding of halogen production in the Arctic.

The production of Br_2 is quite complex and is dependent on many factors, including the relative concentrations of bromide and chloride (among others), the availability of atmospheric

780   oxidants, such as ozone (e.g., Oum et al., 1998; Pratt et al., 2013), the pH of the snow surfaces or

781   aerosol (Toyota et al., 2011, 2014), the presence of snow phase oxidants such as H_2O_2 (Pratt et

782   al., 2013), and the replenishment of the snowpack halides from deposited sea salts. The last of

783   these is governed by meteorology, the proximity of open water or saline sea ice surfaces, and

784   wind/storm events, making the accurate modeling of these processes very complex (Domine et

785   al., 2013). Likewise, to date, it has not been possible to determine the halide concentrations or

786   pH of the snow grain surfaces, and these values are likely highly variable and dependent on snow

787   and aerosol aging and deposition of atmospheric constituents. Due to the apparent importance of

788   surface chemistry for both the initiation and evolution of Arctic ozone depletion events, it is clear

789   that more laboratory and field studies are required to decipher these complex chemical and

790   physical processes.   In particular, we strongly recommend studies relating to direct

791   measurements of surface fluxes of molecular halogens, as a function of conditions of temperature,

792   snowpack composition, and pH, as well as deposition velocities for the hypohalous acids (HOBr,

793   HOCl) to the snow. Our model overestimation of HOBr, that necessitated constraint to

794   observations, suggests a sometimes much stronger, but also variable, deposition of HOBr that is

795   currently unknown.   Further, there is currently little understanding of the mechanism for Cl_2

796   production in the Arctic, and no successful measurements of IO in the High Arctic.   Recent

797   observations of I_2 within the Barrow snowpack (Raso et al., 2016) suggest reactive iodine

798   chemistry is present in this region, and this would have an impact on Br recycling and ozone

799   depletion rate. Investigations into these areas would greatly increase our understanding of

800   halogen chemistry and ozone depletion in the Arctic.

801

References

Abbatt, J., Oldridge, N., Symington, A., Chukalovskiy, V., McWhinney, R. D., Sjostedt, S. and Cox, R. A.: Release of Gas-Phase Halogens by Photolytic Generation of OH in Frozen Halide−Nitrate Solutions: An Active Halogen Formation Mechanism?, J. Phys. Chem. A, 114(23), 6527–6533, doi:10.1021/jp102072t, 2010.

Abbatt, J. P. D., Thomas, J. L., Abrahamsson, K., Boxe, C., Granfors, A., Jones, A. E., King, M. D., Saiz-Lopez, A., Shepson, P. B., Sodeau, J., Toohey, D. W., Toubin, C., von Glasow, R., Wren, S. N., and Yang, X.: Halogen activation via interactions with environmental ice and snow in the polar lower troposphere and other regions, Atmos. Chem. Phys., 12, 6237-6271, 2012.

Adams, J., Holmes, N., and Crowley, J.: Uptake and reaction of HOBr on frozen and dry NaCl/NaBr surfaces between 253 and 233K, Atmos. Chem. Phys., 2, 79 − 91, doi: 10.5194/acp-2-79-2002, 2002.

Ariya, P., Jobson, B., Sander, R., Niki, H., Harris, G., Hopper, J., and Anlauf, K.: Measurements of C2-C7 hydrocarbons during the Polar Sunrise Experiment 1994: Further evidence for halogen chemistry in the troposphere, J. Geophys. Res., 103, 13169-13180, 1998.

Atkinson, R., Baulch, D. L., Cox, R. A., Crowley, J. N., Hampson, R. F., Hynes, R. G., Jenkin, M. E., Rossi, M. J. and Troe, J.: Evaluated kinetic and photochemical data for atmospheric chemistry: Volume II gas phase reactions of organic species, Atmos. Chem. Phys., 6, 3625-4055, 2006.

Atkinson, R., Baulch, D. L., Cox, R. A., Crowley, J. N., Hampson, R. F., Hynes, R. G., Jenkin, M. E., Rossi, M. J. and Troe, J.: Evaluated kinetic and photochemical data for atmospheric chemistry: Volume III gas phase reactions of inorganic halogens, Atmos. Chem. Phys., 7, 981-119, 2007.

840 Barrie, L., Bottenheim, J., Schnell, R., Crutzen, P., and Rasmussen, R.: Ozone destruction and
841 photochemical reactions at polar sunrise in the lower Arctic atmosphere, Nature, 334, 138 - 141,
842 doi: 10.1038/334138a0, 1988.

844 Bottenheim, J.W., Barrie, L. A., Atlas, E., Heidt, L. E., Niki, H., Rasmussen, R. A., and Shepson,
845 P.B.: Depletion of lower tropospheric ozone during Arctic spring: The Polar Sunrise Experiment
846 1998, J. Geophys. Res., 95, 18555-18568, 1990.

848 Calvert, J. G., and Lindberg, S. E.: Potential influence of iodine-containing compounds on the
849 chemistry of the troposphere in the polar spring. I. Ozone depletion, Atmos. Environ., 38, 5087-
850 5104, doi: 10.1016/j.atmosenv.2004.05.049, 2004.

852 Cao, L., Sihler, H., Platt, U., and Gutheil, E.: Numerical analysis of the chemical kinetic
853 mechanisms of ozone depletion and halogen release in the polar troposphere, Atmos. Chem.
854 Phys., 14, 3771-3787, 2014.

856 Carpenter, L. J., S. M. MacDonald, M. D. Shaw, R. Kumar, R.W. Saunders, R. Parthipan,
857 J.Wilson and J. M. C. Plane, Atmospheric iodine levels influenced by sea surface emissions of
858 inorganic iodine, Nature Geosci., 6, 108-111, doi: 10.1038/ngeo1687, 2013.

859 Cavender, A., Biesenthal, T., Bottenheim, J., and Shepson, P.: Volatile organic compound ratios
860 as probes of halogen atom chemistry in the Arctic, Atmos. Chem. Phys., 8, 1737-1750, 2008.

862 Custard, K. D., Thompson, C. R., Pratt, K. A., Shepson, P. B., Liao, J., Huey, L. G., Orlando, J.
863 J., Weinheimer, A. J., Apel, E., Hall, S. R., Flocke, F., Mauldin, L., Hornbrook, R. S., Pöhler, D.,
864 General, S., Zielcke, J., Simpson, W. R., Platt, U., Fried, A., Weibring, P., Sive, B. C., Ullmann,
865 K., Cantrell, C., Knapp, D. J., and Montzka, D. D.: The NOx dependence of bromine chemistry
866 in the Arctic atmospheric boundary layer, Atmos. Chem. Phys., 15, 10799-10809, 2015.

868 Domine, F., J. Bock, D. Voisin, and D. J. Donaldson, Can We Model Snow Photochemistry?
869 Problems with the Current Approaches, J. Phys. Chem., A, 117, 4733−4749, doi:
870 10.1021/jp3123314, 2013.

872 Edwards, G. D., Cantrell, C. A., Stephens, S., Hill, B., Goyea, O., Shetter, R. E., Mauldin III, R.
873 L., Kosciuch, E., Tanner, D. J., and Eisele, F. L.: Chemical ionization mass spectrometer
874 instrument for the measurement of tropospheric HO_2 and RO_2, Anal. Chem., 75, 5317-5327, doi:
875 10.1021/ac034402b, 2003.

877 Ehhalt, D. H.: Photooxidation of trace gases in the troposphere Plenary Lecture, Phys. Chem.
878 Chem. Phys., 1, 5401-5408, 1999.

880 Fan, S-M. and D. J. Jacob, Surface ozone depletion in Arctic spring sustained by bromine
881 reactions on aerosols, Nature, 358, 522-524, 1992.

883 Foster, K. L., Plastridge, R. A., Bottenheim, J. W., Shepson, P. B., Finlayson-Pitts, B. J., and
884 Spicer, C. W.: The role of Br_2 and BrCl in surface ozone destruction at polar sunrise, Science,
885 291, 471-474, 2001.

886
887 Frieß, U., Deutschmann, T., Gilfedder, B., Weller, R., and Platt, U.: Iodine monoxide in the
888 Antarctic snowpack, Atmos. Chem. Phys, 10, 2439-2456, 2010.
889
890 Gladich, I., J. S. Francisco, R. J. Buszek, M. Vazdar, M. A. Caignano, and P. B. Shepson, *Ab*
891 *Initio* Study of the Reaction of Ozone with Bromide Ion, J. Phys. Chem. A, 119, 4482−4488,
892 2015.
893
894 Gong, S., Walmsley, J., Barrie, L., and Hopper, J.: Mechanisms for surface ozone depletion and
895 recovery during polar sunrise, Atmos. Environ., 31, 969-981, 1997.
896
897 Guimbaud, C., Grannas, A. M., Shepson, P. B., Fuentes, J. D., Boudries, H., Bottenheim, J. W.,
898 Dominé, F., Houdier, S., Perrier, S., and Biesenthal, T. B.: Snowpack processing of acetaldehyde
899 and acetone in the Arctic atmospheric boundary layer, Atmos. Environ., 36, 2743-2752, 2002.
900
901 Hausmann, M., and Platt, U.: Spectroscopic measurement of bromine oxide and ozone in the
902 high Arctic during Polar Sunrise Experiment 1992, J. Geophys. Res., 99, 25399, 1994.
903
904 Helmig, D., Ganzeveld, L., Butler, T., and Oltmans, S.: The role of ozone atmosphere-snow gas
905 exchange on polar, boundary-layer tropospheric ozone? a review and sensitivity analysis, Atmos.
906 Chem. Phys., 7, 15-30, 2007.
907
908 Helmig, D., Boylan, P., Johnson, B., Oltmans, S., Fairall, C., Staebler, R., Weinheimer, A.,
909 Orlando, J., Knapp, D. J., Montzka, D. D., Flocke, F., Frieß, U., Sihler, H., and Shepson, P. B.:
910 Ozone dynamics and snow-atmosphere exchanges during ozone depletion events at Barrow,
911 Alaska, J. Geophys. Res., 117, D20303, doi:10.1029/2012JD017531, 2012.
912
913 Hirokawa, J., Onaka, K., Kajii, Y., and Akimoto, H.: Heterogeneous processes involving sodium
914 halide particles and ozone: molecular bromine release in the marine boundary layer in the
915 absence of nitrogen oxides, Geophys. Res. Lett., 25, 2449-2452, 1998.
916
917 Holmes, C. D., Jacob, D. J., Corbitt, E. S., Mao, J., Yang, X., Talbot, R., and Slemr, F.: Global
918 atmospheric model for mercury including oxidation by bromine atoms, Atmos. Chem. Phys., 10,
919 12037-12057, 2010.
920
921 Hönninger, G.: Halogen Oxide Studies in the Boundary Layer by Multi Axis Differential Optical
922 Absorption Spectroscopy and Active Longpath-DOAS, Ph.D., University of Heidelberg, 2002.
923
924 Huff, A. K., and Abbatt, J. P. D.: Kinetics and product yields in the heterogeneous reactions of
925 HOBr with ice surfaces containing NaBr and NaCl, J. Phys. Chem. A, 106, 5279-5287, 2002.
926
927 Jacob, D. J.: Heterogeneous chemistry and tropospheric ozone, Atmos. Environ., 34, 2131-2159,
928 2000.
929

930 Jobson, B., Niki, H., Yokouchi, Y., Bottenheim, J., Hopper, F., and Leaitch, R.: Measurements
931 of C2-C6 hydrocarbons during the Polar Sunrise 1992 Experiment: Evidence for Cl atom and Br
932 atom chemistry, J. Geophys. Res., 99, 25355-25368, 1994.
933
934 Kukui, A., Kirchner, U., Benter, T., and Schindler, R. N.: A gas kinetic investigation of HOBr
935 reactions with $Cl(^2P)$, $O(^3P)$ and $OH(^2II)$. The reaction of BrCl with $OH(^2II)$, Berichte Der
936 Bunsen-Gesellschaft-Physical Chemistry Chemical Physics, 100, 455-461, 1996.
937
938 Kuo, K. K.: Principles of combustion, John Wiley & Sons, New York, 1986.
939
940 Lary, D.: Gas phase atmospheric bromine photochemistry, J. Geophys. Res., 101, 1505-1516,
941 1996.
942
943 Le Bras, G., and Platt, U.: A possible mechanism for combined chlorine and bromine catalyzed
944 destruction of tropospheric ozone in the Arctic, Geophys. Res. Lett., 22, 599-602, 1995.
945
946 Lehrer, E., Hönninger, G., and Platt, U.: A one dimensional model study of the mechanism of
947 halogen liberation and vertical transport in the polar troposphere, Atmos. Chem. Phys., 4, 2427-
948 2440, 2004.
949
950 Liao, J., Huey, L., Scheuer, E., Dibb, J., Stickel, R., Tanner, D., Neuman, J., Nowak, J., Choi, S.,
951 and Wang, Y.: Characterization of soluble bromide measurements and a case study of BrO
952 observations during ARCTAS, Atmos. Chem. Phys, 12, 1327-1338, 2012a.
953
954 Liao, J., Huey, L., Tanner, D., Flocke, F., Orlando, J., Neuman, J., Nowak, J., Weinheimer, A.,
955 Hall, S., Smith, J., Fried, A., Staebler, R., Wang, Y., Koo, J.-H., Cantrell, C., Weibring, P.,
956 Walega, J., Knapp, D., Shepson, P., and Stephens, C.: Observations of inorganic bromine (HOBr,
957 BrO, and Br_2) speciation at Barrow, Alaska, in spring 2009, J. Geophys. Res., 117, D00R16,
958 2012b.
959
960 Liao, J., L. G. Huey, Z. Liu, D. J. Tanner, C. A. Cantrell, J. J. Orlando, F. M. Flocke, P. B.
961 Shepson, A. J. Weinheimer, S. R. Hall, H. J. Beine, Y. Wang, E. D. Ingall, C. R. Stephens, R. S.
962 Hornbrook, E. Apel, A. Fried, L. Mauldin, J. N. Smith, R. M. Staebler, J.A. Neuman, J.B.
963 Nowak, High levels of molecular chlorine in the Arctic atmosphere, Nature Geosci., 7, 91 – 94,
964 doi:10.1038/ngeo2046, 2014.
965 Mahajan, A., Shaw, M., Oetjen, H., Hornsby, K., Carpenter, L., Kaleschke, L., Tian-Kunze, X.,
966 Lee, J., Moller, S., and Edwards, P.: Evidence of reactive iodine chemistry in the Arctic
967 boundary layer, J. Geophys. Res., 115, D20303, doi: 10.1029/2009JD013665, 2010.
968
969 Mallard, W. G., Westley, F., Herron, J. T., Hampson, R. F., and Frizzel, D. H.: NIST Chemical
970 Kinetics Database: Version 5.0 National Institute of Standards and Technology, Gaithersburg,
971 MD. , 1993.
972

973 Martinez, M., Arnold, T., and Perner, D.: The role of bromine and chlorine chemistry for arctic
974 ozone depletion events in Ny-Ålesund and comparison with model calculations, Annales
975 Geophysicae, 17, 941-956, 1999.

977 McFiggans, G., Plane, J. M. C., Allan, B. J., Carpenter, L. J., Coe, H., and O'Dowd, C.: A
978 modeling study of iodine chemistry in the marine boundary layer, J. Geophys. Res., 105, 14371-
979 14385, 2000.

981 McFiggans, G., Cox, R. A., Mössinger, J. C., Allan, B. J., and Plane, J. M. C.: Active chlorine
982 release from marine aerosols: Roles for reactive iodine and nitrogen species, J. Geophys. Res,
983 107, doi: 10.1029/2001JD000383, 2002.

985 Michalowski, B. A., Francisco, J. S., Li, S. M., Barrie, L. A., Bottenheim, J. W., and Shepson, P.
986 B.: A computer model study of multiphase chemistry in the Arctic boundary layer during polar
987 sunrise, J. Geophys. Res., 105, 15131 – 15145, 2000.

989 Mielke, L. H., Furgeson, A., and Osthoff, H. D.: Observation of $ClNO_2$ in a mid-continental
990 urban environment, Environ. Sci. Technol., 45, 8889-8896, 2011.

992 Monks, P. S.: Gas-phase radical chemistry in the troposphere, Chem. Soc. Rev., 34, 376-395,
993 2005.

995 Neuman, J. A., Nowak, J. B., Huey, L. G., Burkholder, J. B., Dibb, J. E., Holloway, J. S., Liao, J.,
996 Peischl, J., Roberts, J. M., Ryerson, T. B., Scheuer, E., Stark, H., Stickel, R. E., Tanner, D. J.,
997 and Weinheimer, A.: Bromine measurements in ozone depleted air over the Arctic Ocean, Atmos.
998 Chem. Phys., 10, 6503-6514, 2010.

1000 Oum, K., Lakin, M., DeHaan, D., Brauers, T., and Finlayson-Pitts, B.: Formation of molecular
1001 chlorine from the photolysis of ozone and aqueous sea-salt particles, Science, 279, 74, 1998a.

1003 Oum, K., Lakin, M., and Finlayson-Pitts, B.: Bromine activation in the troposphere by the dark
1004 reaction of O_3 with seawater ice, Geophys. Res. Lett., 25, 3923-3926, 1998b.

1006 Papanastasiou, D.K., McKeen, S. A., and Burkholder, J. B.: The very short-lived ozone depleting
1007 substance CHBr3 (bromoform): revised UV absorption spectrum, atmospheric lifetime, and
1008 ozone depletion potential, Atmos. Chem. Phys., 14, 3017 – 3025, 2014.

1010 Piot, M., and Von Glasow, R.: The potential importance of frost flowers, recycling on snow, and
1011 open leads for ozone depletion events, Atmos. Chem. Phys., 8, 2437-2467, 2008.

1013 Platt, U., and Janssen, C.: Observation and role of the free radicals NO_3, ClO, BrO and IO in the
1014 troposphere, Faraday Discuss., 100, 175-198, 1995.

1016 Pöhler, D., Vogel, L., Frieß, U., and Platt, U.: Observation of halogen species in the Amundsen
1017 Gulf, Arctic, by active long-path differential optical absorption spectroscopy, Proceedings of the
1018 National Academy of Sciences, 107, 6582, 2010.

1019

1020   Pratt, K. A., Custard, K. D., Shepson, P. B., Douglas, T. A., Pöhler, D., General, S., Zielcke, J.,
1021   Simpson, W. R., Platt, U., Tanner, D. J., Huey, L. G., Carlsen, M., and Stirm, B. H.:
1022   Photochemical production of molecular bromine in Arctic surface snowpacks, Nature Geosci., 6,
1023   351 – 356, doi: 10.1038/ngeo1779, 2013.

1024

1025   Raso, A. R. W., Custard, K. D., Pratt, K. A., Tanner, D. J., Huey, L. G., and Shepson, P. B.:
1026   Active molecular iodine snowpack photochemistry in the Arctic, Proc. Nat. Acad. Sci., submitted,
1027   2016.

1028

1029   Saiz-Lopez, A., Mahajan, A. S., Salmon, R. A., Bauguitte, S. J. B., Jones, A. E., Roscoe, H. K.,
1030   and Plane, J. M. C.: Boundary layer halogens in coastal Antarctica, Science, 317, 348-351, 2007.

1031

1032   Saiz-Lopez, A., Plane, J. M. C., Mahajan, A. S., Anderson, P. S., Bauguitte, S. J. B., Jones, A. E.,
1033   Roscoe, H. K., Salmon, R. A., Bloss, W. J., and Lee, J. D.: On the vertical distribution of
1034   boundary layer halogens over coastal Antarctica: implications for O_3, HO_x, NO_x and the Hg
1035   lifetime, Atmos. Chem. Phys., 8, 887-900, 2008.

1036

1037   Sander, R., Keene, W. C., Pszenny, A. A. P., Arimoto, R., Ayers, G. P., Baboukas, E., Cainey, J.
1038   M., Crutzen, P. J., Duce, R. A., Hönninger, G., Huebert, B. J., Maenhaut, W., Mihalopoulos, N.,
1039   Turekian, C., and van Dingenen, R.: Inorganic bromine in the marine boundary layer: a critical
1040   review, Atmos. Chem. Phys., 3, 1301-1336, 2003.

1041

1042   Shetter, R. E., and Müller, M.: Photolysis frequency measurements using actinic flux
1043   spectroradiometry during the PEM-Tropics mission: Instrumentation description and some
1044   results, J. Geophys. Res., 104, 5647-5661, 1999.

1045

1046   Shepson, P. B., Sirju, A.-P., Hopper, J. F., Barrie, L. A., Young, V., Niki, H. and Dryfhout, H.:
1047   Sources and sinks of carbonyl compounds in the Arctic Ocean boundary layer: a polar ice floe
1048   experiment, J. Geophys. Res., 101, 21081 - 21089, 1996.

1049

1050   Staebler, R. M., den Hartog, G., Georgi, B., and Sterdiek, T. D.: Aerosol size distribution in
1051   Arctic haze during the Polar Sunrise Experiment 1992, J. Geophys. Res., 99, 25429-25437, 1994.

1052

1053   Sumner, A. L., and Shepson, P. B.: Snowpack production of formaldehyde and its effect on the
1054   Arctic troposphere, Nature, 398, 230-233, 1999.

1055

1056   Stephens, C. R., Shepson, P. B., Steffen, A., Bottenheim, J. W., Liao, J., Huey, L. G., Apel, E.,
1057   Weinheimer, A., Hall, S. R., and Cantrell, C.: The relative importance of chlorine and bromine
1058   radicals in the oxidation of atmospheric mercury at Barrow, Alaska, J. Geophys. Res., 117,
1059   D00R11, doi: 10.1029/2011JD016649, 2012.

1060

1061   Sturges, W., and Barrie, L.: Chlorine, bromine and iodine in Arctic aerosols, Atmos. Environ., 22,
1062   1179-1194, 1988.

1063

Tang, T., and McConnell, J.: Autocatalytic release of bromine from Arctic snow pack during polar sunrise, Geophys. Res. Lett., 23, 2633-2636, 1996.

Thomas, J. L., Stutz, J., Lefer, B., Huey, L. G., Toyota, K., Dibb, J. E., and von Glasow, R.: Modeling chemistry in and above snow at Summit, Greenland – Part 1: Model description and results, Atmos. Chem. Phys., 11, 4899-4914, 2011.

Thompson, C. R., Shepson, P. B., Liao, J., Huey, L. G., Apel, E. C., Cantrell, C. A., Flocke, F., Orlando, J., Fried, A., Hall, S. R., Hornbrook, R. S., Knapp, D. J., Mauldin III, R. L., Montzka, D. D., Sive, B. C., Ullmann, K., Weibring, P. and Weinheimer, A.: Interactions of bromine, chlorine, and iodine photochemistry during ozone depletions in Barrow, Alaska, Atmos. Chem. Phys., 15, 9651 – 9679, doi: 10.5194/acp-15-9651-2015, 2015.

Thornton, J. A., Kercher, J. P., Riedel, T. P., Wagner, N. L., Cozic, J., Holloway, J. S., Dubé, W. P., Wolfe, G. M., Quinn, P. K., Middlebrook, A. M., Alexander, B., and Brown, S. S.: A large atomic chlorine source inferred from mid-continental reactive nitrogen chemistry, Nature, 464, 271-274, 2010.

Toyota, K., McConnell, J. C., Lupu, A., Neary, L., McLinden, C. A., Richter, A., Kwok, R., Semeniuk, K., Kaminski, J. W., Gong, S. –L., Jarosz, J., Chipperfield, M. P., and Sioris, C. E.: Analysis of reactive bromine production and ozone depletion in the Arctic boundary layer using 3-D simulations with GEM-AQ: inference from synoptic-scale patterns, Atmos. Chem. Phys., 11, 3949-3979, 2011.

Toyota, K., McConnell, J. C., Staebler, R. M., and Dastoor, A. P.: Air-snowpack exchange of bromine, ozone and mercury in the springtime Arctic simulated by the 1-D model PHANTAS - Part 1: In-snow bromine activation and its impact on ozone, Atmos. Chem. Phys., 14, 4101-4133, 2014.

Vogt, R., Crutzen, P. J., and Sander, R.: A mechanism for halogen release from sea-salt aerosol in the remote marine boundary layer, Nature, 383, 327 – 330, doi: 10.1038/383327a0, 1996.

Vogt, R., Sander, R., von Glasow, R., and Crutzen, P. J.: Iodine chemistry and its role in halogen activation and ozone loss in the marine boundary layer: A model study, J. Atmos. Chem., 32, 375-395, 1999.

Wennberg, P., Hanisco, T., Jaegle, L., Jacob, D., Hintsa, E., Lanzendorf, E., Anderson, J., Gao, R. S., Keim, E., and Donnelly, S.: Hydrogen radicals, nitrogen radicals, and the production of O_3 in the upper troposphere, Science, 279, 49-53, 1998.

Young, C. J., Washenfelder, R. A., Roberts, J. M., Mielke, L. H., Osthoff, H. D., Tsai, C., Pikelnayai, O., Stutz, J., Veres, P. R., Cochran, A. K., VandenBoer, T. C., Flynn, J., Grossberg, N., Haman, C. L., Lefer, B., Stark, H., Graus, M., de Gouw, J., Gilman, J. B., Kuster, W. C., and Brown, S. S.: Vertically resolved measurements of nighttime radical reservoirs in Los Angeles and their contribution to the urban radical budget, Environ. Sci. Technol., 46, 10965-10973, 2012.

1110   Zeng, T., Wang, Y., Chance, K., Blake, N., Blake, D., and Ridley, B.: Halogen-driven low-
1111   altitude O_3 and hydrocarbon losses in spring at northern high latitudes, J. Geophys. Res, 111,
1112   D17, doi: 10.1029/2005JD006706, 2006.

1113

1114 **Table 1.** Reactions used in the model that are pertinent to bromine chemistry. All rate constants
1115 (with the exception of photolysis J coefficients) are in units of cm^3 molecule^{-1} s^{-1}.
1116

Gas-Phase Reactions	Rate Constant	Reference
1117		
1118 $Br + O_3 \rightarrow BrO$	6.75×10^{-13}	*Atkinson et al.* [2004]
1119 $Br + C_2H_4 \rightarrow HBr + C_2H_5OO$	1.3×10^{-13}	*Atkinson et al.* [2004]
1120 $Br + C_3H_6 \rightarrow HBr + C_3H_5$	1.60×10^{-12}	*Atkinson et al.* [2004]
1121 $Br + HCHO \rightarrow HBr + CO + HO_2$	6.75×10^{-13}	*Sander et al.* [2006]
1122 $Br + CH_3CHO \rightarrow HBr + CH_3COOO$	2.8×10^{-12}	*Atkinson et al.* [2004]
1123 $Br + C_3H_6O \rightarrow HBr$	9.7×10^{-12}	*Wallington et al.* [1989]
1124 $Br + nButanal \rightarrow HBr$	9.7×10^{-12}	estimate from *Michalowski et al.* [2000]
1125 $Br + CH_3OOH \rightarrow HBr + CH_3OO$	4.03×10^{-15}	*Mallard et al.* [1993]
1126 $Br + NO_2 \rightarrow BrNO_2$	2.7×10^{-11}	*Atkinson et al.* [2004]
1127 $Br + BrNO_3 \rightarrow Br_2 + NO_3$	4.9×10^{-11}	*Orlando and Tyndall* [1996]
1128 $Br + OClO \rightarrow BrO + ClO$	1.43×10^{-13}	*Atkinson et al.* [2004]
1129 $BrO + O(^3P) \rightarrow Br$	4.8×10^{-11}	*Atkinson et al.* [2004]
1130 $BrO + OH \rightarrow Br + HO_2$	4.93×10^{-11}	*Atkinson et al.* [2004]
1131 $BrO + HO_2 \rightarrow HOBr$	3.38×10^{-11}	*Atkinson et al.* [2004]
1132 $BrO + CH_3OO \rightarrow HOBr + CH_2OO$	4.1×10^{-12}	*Aranda et al.* [1997]
1133 $BrO + CH_3OO \rightarrow Br + HCHO + HO_2$	1.6×10^{-12}	*Aranda et al.* [1997]
1134 $BrO + CH_3COOO \rightarrow Br + CH_3COO$	1.7×10^{-12}	estimate from *Michalowski et al.* [2000]
1135 $BrO + C_3H_6O \rightarrow HOBr$	1.5×10^{-14}	estimate from *Michalowski et al.* [2000]
1136 $BrO + NO \rightarrow Br + NO_2$	2.48×10^{-11}	*Atkinson et al.* [2004]
1137 $BrO + NO_2 \rightarrow BrNO_3$	1.53×10^{-11}	*Atkinson et al.* [2004]
1138 $BrO + BrO \rightarrow Br + Br$	2.82×10^{-12}	*Sander et al.* [2006]
1139 $BrO + BrO \rightarrow Br_2$	9.3×10^{-13}	*Sander et al.* [2006]
1140 $BrO + HBr \rightarrow HOBr + Br$	2.1×10^{-14}	*Hansen et al.* [1999]
1141 $HBr + OH \rightarrow Br + H_2O$	1.26×10^{-11}	*Sander et al.* [2006]
1142 $CH_3Br + OH \rightarrow H_2O + Br$	1.27×10^{-14}	*Atkinson et al.* [2004]
1143 $CHBr_3 + OH \rightarrow H_2O + Br$	1.2×10^{-13}	*Atkinson et al.* [2004]
1144 $Cl + BrCl \leftarrow\rightarrow Br + Cl_2$	f: 1.5×10^{-11} r: 1.1×10^{-15}	*Clyne et al.* [1972]
1145 $Cl + Br_2 \leftarrow\rightarrow BrCl + Br$	f: 1.2×10^{-10} r: 3.3×10^{-15}	*Clyne et al.* [1972]
1146 $BrO + ClO \rightarrow Br + Cl$	7.04×10^{-12}	*Atkinson et al.* [2004]
1147 $BrO + ClO \rightarrow BrCl$	1.15×10^{-12}	*Atkinson et al.* [2004]
1148 $BrO + ClO \rightarrow Br + OClO$	9.06×10^{-12}	*Atkinson et al.* [2004]
1149 $HOBr + OH \rightarrow BrO + H_2O$	5.0×10^{-13}	*Kukui et al.* [1996]
1150 $HOBr + Cl \rightarrow BrCl + OH$	8.0×10^{-11}	*Kukui et al.* [1996]
1151 $HOBr + O(^3P) \rightarrow BrO + OH$	2.12×10^{-11}	*Atkinson et al.* [2004]
1152 $IO + BrO \rightarrow Br + OIO$	9.36×10^{-11}	*Atkinson et al.* [2004]
1153 $IO + BrO \rightarrow IBr$	4.32×10^{-11}	*Atkinson et al.* [2004]
1154 $IO + BrO \rightarrow Br + I$	7.2×10^{-12}	*Atkinson et al.* [2004]

1155

Photolysis Reactions	J_{max} (25 March) s^{-1}	Lifetime	Reference
1157 $BrNO_3 \rightarrow Br + NO_3$	2.1×10^{-4}	1.3 h	calculated from OASIS data
1158 $BrNO_3 \rightarrow BrO + NO_2$	1.2×10^{-3}	14.2 min	calculated from OASIS data
1159 $BrO \rightarrow Br + O(^3P)$	3.0×10^{-2}	33 s	calculated from OASIS data
1160 $Br_2 \rightarrow Br + Br$	4.4×10^{-2}	23 s	calculated from OASIS data
1161 $HOBr \rightarrow Br + OH$	2.3×10^{-3}	7.2 min	calculated from OASIS data
1162 $BrNO_2 \rightarrow Br + NO_2$	1.5×10^{-4}	1.8 h	estimate from *Lehrer et al.* [2004]

| 1163 | BrCl $\rightarrow$ Br + Cl | | 1.26 x 10^{-2} | | 1.3 min | | calculated from OASIS data |

1164
1165

1166	**Mass Transfer Reactions**	k_t **(forward)**	k_t **(reverse)**
1167	HBr$_{(g)}$ $\rightarrow$ H$^+_{(p)}$ + Br$^-_{(p)}$	1.80 x 10^{-3}	
1168	HCl$_{(g)}$ $\rightarrow$ H$^+_{(p)}$ + Cl$^-_{(p)}$	2.58 x 10^{-3}	
1169	HOBr$_{(g)}$ $\rightarrow$ HOBr$_{(p)}$	1.26 x 10^{-3}	
1170	BrNO$_{2(g)}$ $\rightarrow$ BrNO$_{2(p)}$	1.26 x 10^{-3}	
1171	BrONO$_{3(g)}$ $\rightarrow$ BrONO$_{3(p)}$	1.26 x 10^{-3}	
1172	Br$_{2(g)}$ $\leftrightarrow$ Br$_{2(p)}$	1.78 x 10^{-5}	2.97 x 10^8
1173	BrCl$_{(g)}$ $\leftrightarrow$ BrCl$_{(p)}$	6.60 x 10^{-4}	1.91 x 10^{10}
1174	IBr$_{(p)}$ $\rightarrow$ IBr$_{(g)}$	5.53 x 10^9	
1175	HBr$_{(g)}$ $\rightarrow$ H$^+_{(s)}$ + Br$^-_{(s)}$	1.67 x 10^{-5}	
1176	HCl$_{(g)}$ $\rightarrow$ H$^+_{(s)}$ + Cl$^-_{(s)}$	1.67 x 10^{-5}	
1177	HOBr$_{(g)}$ $\rightarrow$ HOBr$_{(s)}$	1.67 x 10^{-5}	
1178	BrNO$_{2(g)}$ $\rightarrow$ BrNO$_{2(s)}$	1.67 x 10^{-4}	
1179	BrONO$_{3(g)}$ $\rightarrow$ BrONO$_{3(s)}$	1.26 x 10^{-4}	
1180	Br$_{2(g)}$ $\leftrightarrow$ Br$_{2(s)}$	1.0 x 10^{-5}	7.71 x 10^{-2}
1181	BrCl$_{(g)}$ $\leftrightarrow$ BrCl$_{(s)}$	1.25 x 10^{-5}	7.71 x 10^{-2}
1182	IBr$_{(s)}$ $\rightarrow$ IBr$_{(g)}$	7.71 x 10^{-2}	

1183

1184	**Aqueous Phase Reactions**	k **(particle)**	k **(snow)**	**Reference**
1185	Cl$^-$ + HOBr + H$^+$ $\rightarrow$ BrCl	5.17 x 10^{-21}	9.30 x 10^{-26}	*Wang et al.* [1994]
1186	Br$^-$ + HOCl + H$^+$ $\rightarrow$ BrCl	1.2 x 10^{-24}	2.15 x 10^{-29}	*Sander et al.* [1997]
1187	Br$^-$ + HOBr + H$^+$ $\rightarrow$ Br$_2$	1.47 x 10^{-20}	2.64 x 10^{-25}	*Beckwith et al.* [1996]
1188	Br$^-$ + HOI + H$^+$ $\rightarrow$ IBr	3.04 x 10^{-18}	5.46 x 10^{-23}	*Troy et al.* [1991]
1189	BrCl + Cl$^-$ $\rightarrow$ BrCl$_2^-$	3.3	5.99 x 10^{-5}	*Michalowski et al.* [2000]
1190	BrCl$_2^-$ $\rightarrow$ BrCl + Cl$^-$	1.58 x 10^9	1.58 x 10^9	*Michalowski et al.* [2000]
1191	BrCl + Br$^-$ $\rightarrow$ Br$_2$Cl$^-$	3.3	5.99 x 10^{-5}	*Michalowski et al.* [2000]
1192	Br$_2$Cl$^-$ $\rightarrow$ BrCl + Br$^-$	3.34 x 10^5	3.34 x 10^5	*Wang et al.* [1994]
1193	Cl$_2$ + Br$^-$ $\rightarrow$ BrCl$_2^-$	4.27	7.66 x 10^{-5}	*Wang et al.* [1994]
1194	BrCl$_2^-$ $\rightarrow$ Cl$_2$ + Br$^-$	6.94 x 10^2	6.94 x 10^2	*Wang et al.* [1994]
1195	O$_3$ + Br$^-$ $\rightarrow$ HOBr	4.5 x 10^{-9}	8.08 x 10^{-14}	*Oum et al.* [1998]

1196
1197
1198

1199 **Table 2.** Median mid-day bromine chain lengths for 25, 29, and 30 March 2009 (days with O$_3$
1200 present) determined for four different modeling scenarios with different combinations of
1201 halogens present. Method 1 refers to Equation 3 (using terminations reactions) and Method 2
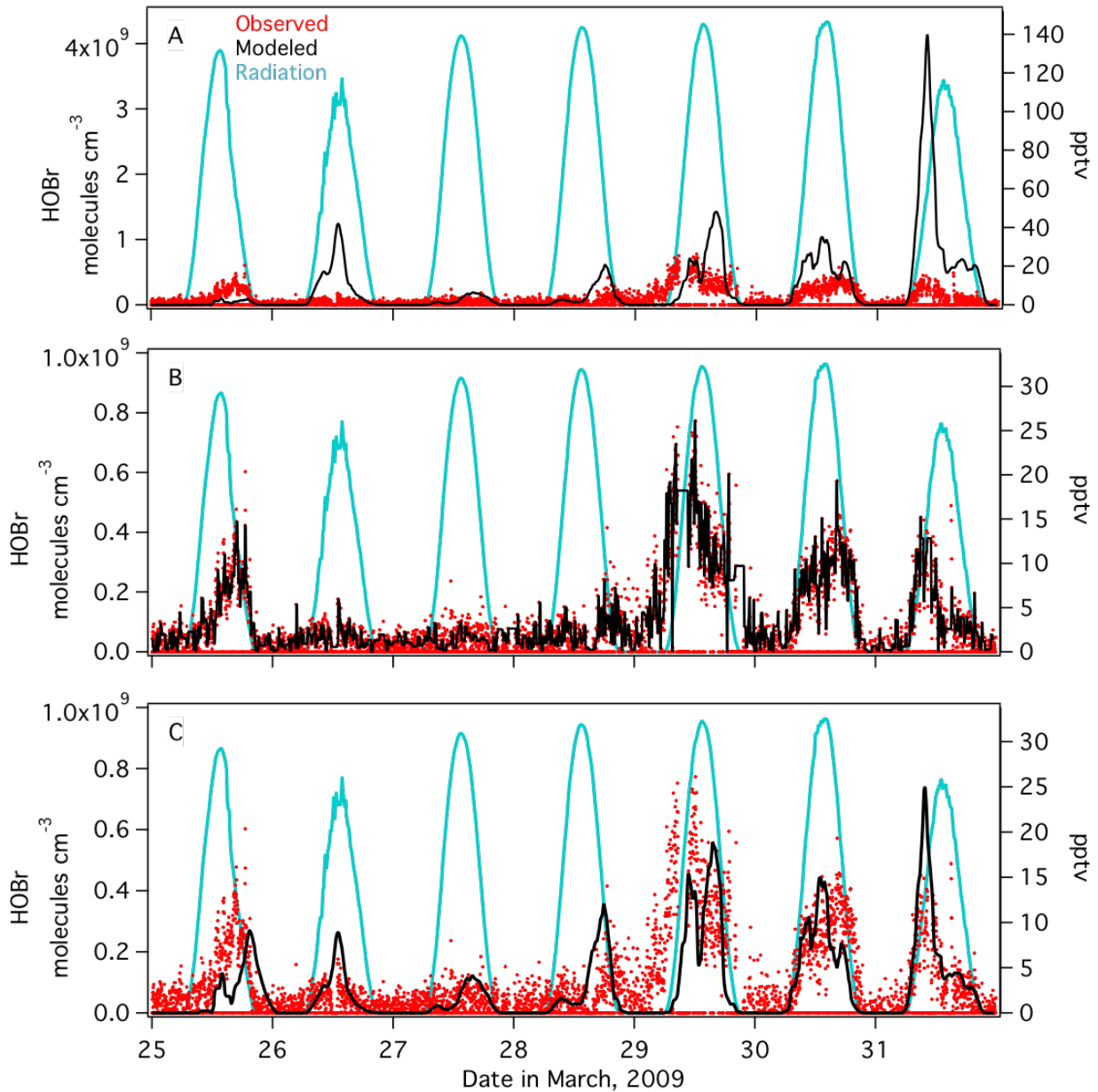1202 refers to Equation 4 (using initiation reactions).

	25 March		29 March		30 March		Average (1-σ st. deviation)	
	Method 1	Method 2	Method 1	Method 2	Method 1	Method 2	Method 1	Method 2
Br only	1.25	0.85	1.51	1.10	1.79	1.40	1.52 (± 0.27)	1.11 (± 0.28)
Br and Cl (Base)	1.29	0.84	1.43	1.03	1.58	1.29	1.43 (± 0.14)	1.05 (± 0.22)
Br and Low I	1.37	0.86	1.60	1.12	1.82	1.41	1.59 (± 0.22)	1.13 (± 0.28)
Br, Cl, and I	1.37	0.87	1.51	1.04	1.65	1.31	1.51 (± 0.14)	1.07 (± 0.23)

1203
1204
1205
1206
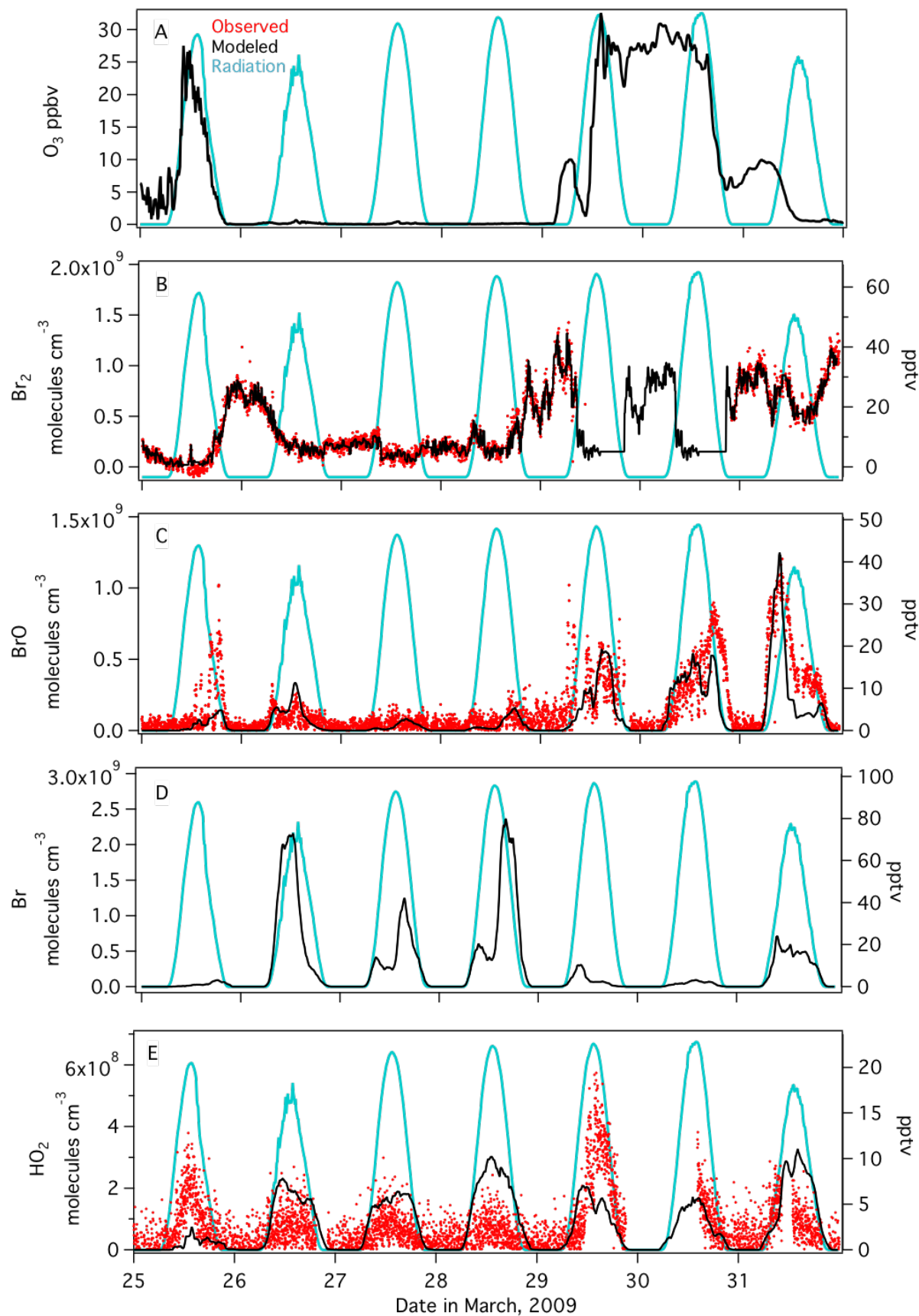
1208
1209 **Fig 1.** Time-series of gas-phase concentrations and mixing ratios of O_3, Br_2, BrO, Br, and HO_2 in
1210 the model (black trace) for the seven-day period simulated. Observations are plotted in red
1211 where available for Br_2, BrO, and HO_2. O_3 and Br_2 are constrained species in the model.
1212 Simulated output of BrO, Br, and HO_2 are smoothed by hourly averaging. Radiation is shown as
1213 the cyan trace as a reference. Time is expressed in Alaska Standard Time.
1214

1215
1216
1217 **Fig 2.** Simulated (black trace) versus observed (red markers) HOBr mixing ratios shown for
1218 three different versions of the model: A) HOBr unconstrained and allowed to freely evolve with
1219 a constant surface deposition term as described in the Methods, B) HOBr constrained to
1220 observations, C) HOBr unconstrained but with a variable surface deposition that is enhanced
1221 during higher wind speeds. Simulated (unconstrained) output in Panels A and C are smoothed by

1222　　hourly averaging. Radiation is shown as the cyan trace as a reference. Time is expressed in
1223　　Alaska Standard Time.
1224
1225
1226
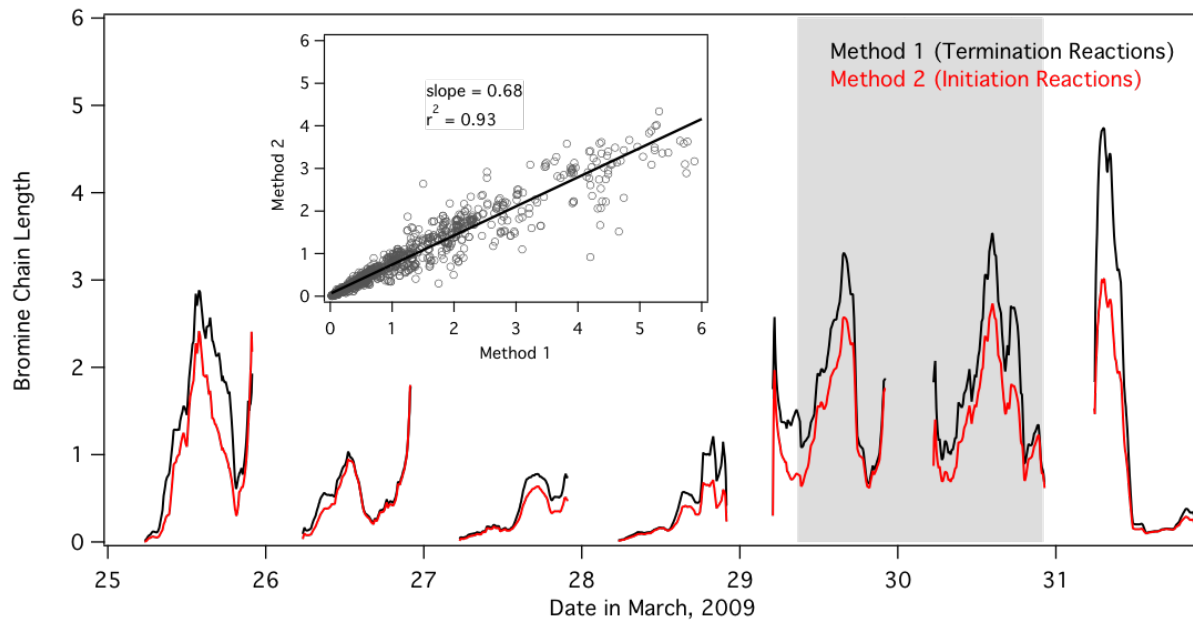
1227

1228　　**Fig 3.** Time-series of model calculated bromine chain length for the daytime hours (7:00 to
1229　　21:00 AKST). Method 1 is plotted as the black trace and Method 2 is plotted as the red trace.
1230　　Model output is smoothed by hourly averaging. The grey shaded box represents a period of
1231　　missing Br_2 observations. The inset graph shows a linear regression of Method 1 and Method 2
1232　　calculations. Time is expressed in Alaska Standard Time.

1233
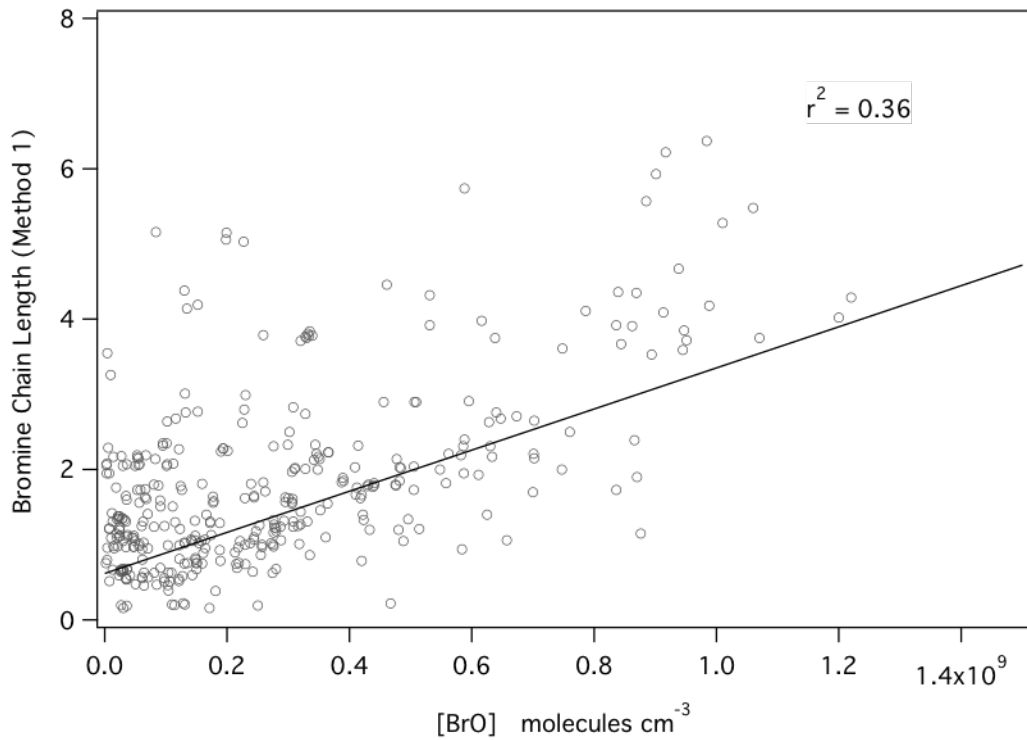
1234

Fig 4. Regression of daytime (7:00 – 21:00 AKST) bromine chain length calculated by Method
1 (Equation 5) and simulated BrO concentration.

1237
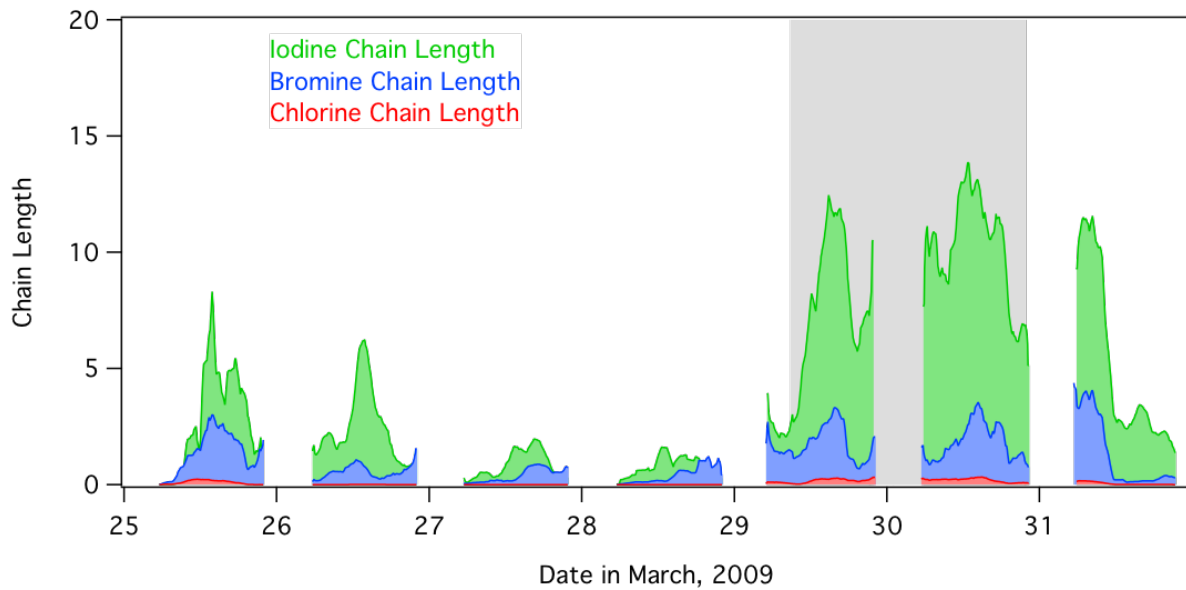
1238

Fig 5. Calculated chain lengths for iodine (green), bromine (blue), and chlorine (red) across the
seven days of the simulated period modeled using the Base + Iodine scenario. Model output is

47

smoothed by hourly averaging. The grey shaded box represents a period of missing Br$_2$
observations. Time is expressed in Alaska Standard Time.
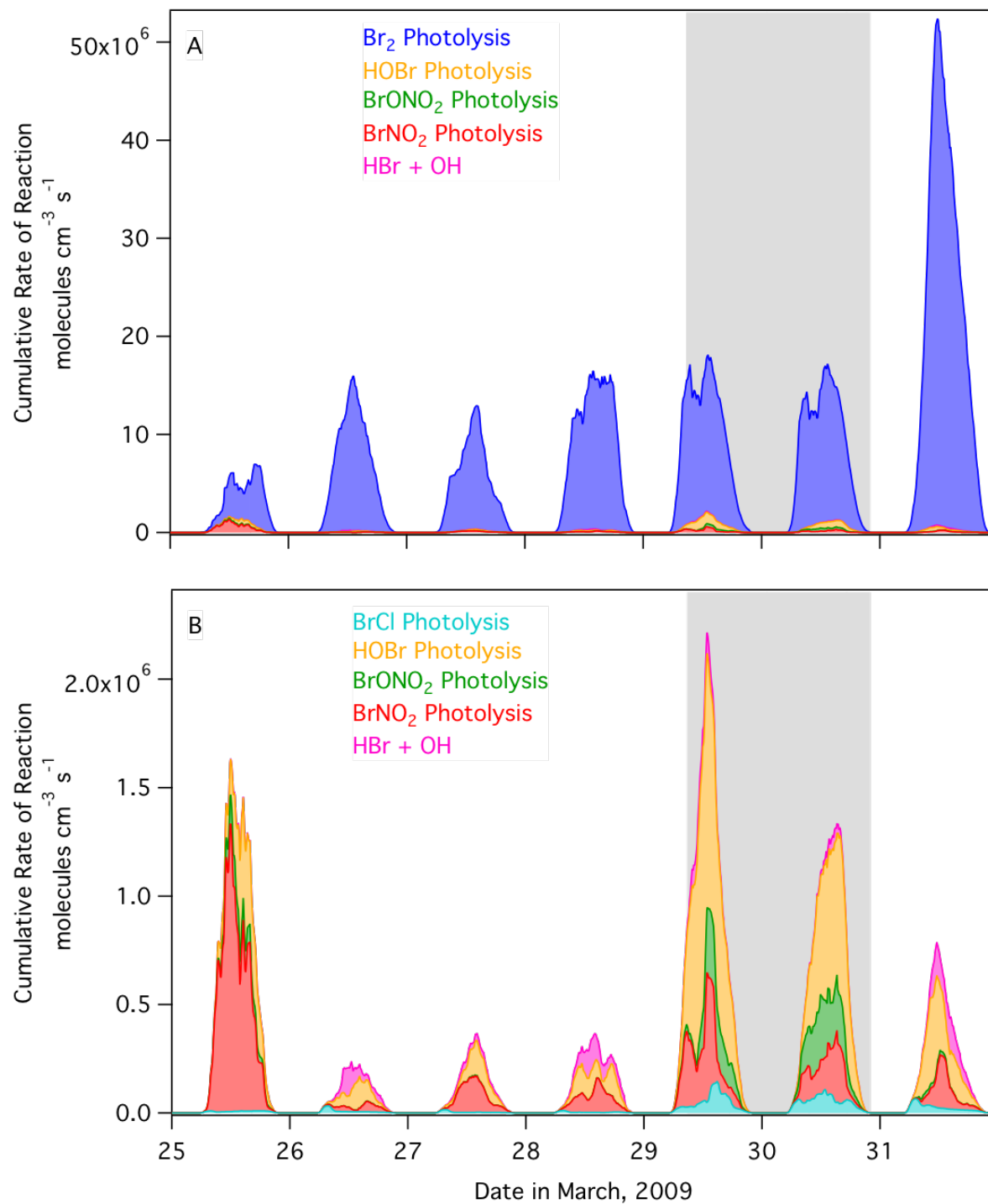
Fig 6. Time-varying rates of the most important bromine initiation reactions in the Base Model.
Panel A includes photolysis of Br$_2$, which dominates the bromine initiation. Br$_2$ photolysis is

1247 calculated as 2 x J_{Br2}[Br_2]. In Panel B, Br_2 photolysis has been removed so that the minor terms
1248 can be visualized. Panel B also includes BrCl, which contributes only a negligible amount to
1249 bromine initiation. Model output is smoothed by hourly averaging. The y-axis is expressed as a
1250 cumulative rate of reaction. The grey shaded box represents a period of missing Br_2 observations.
1251 Time is expressed in Alaska Standard Time.
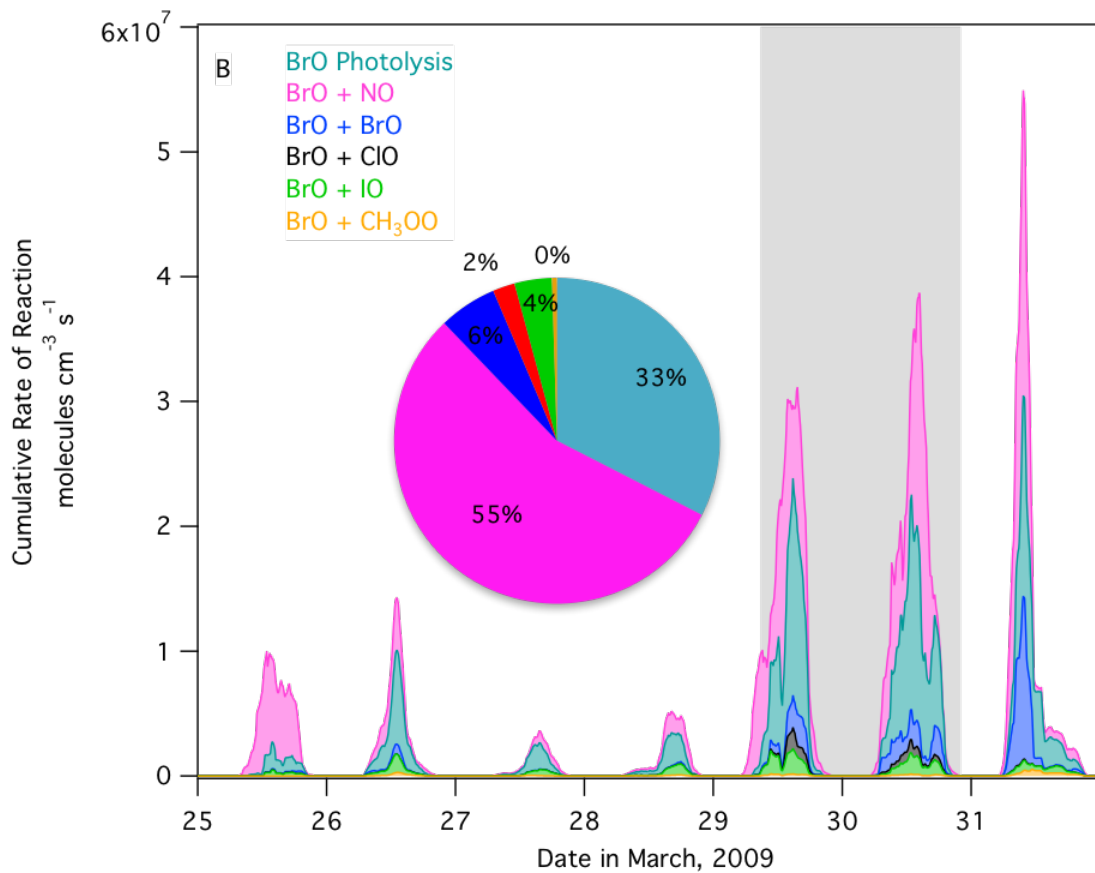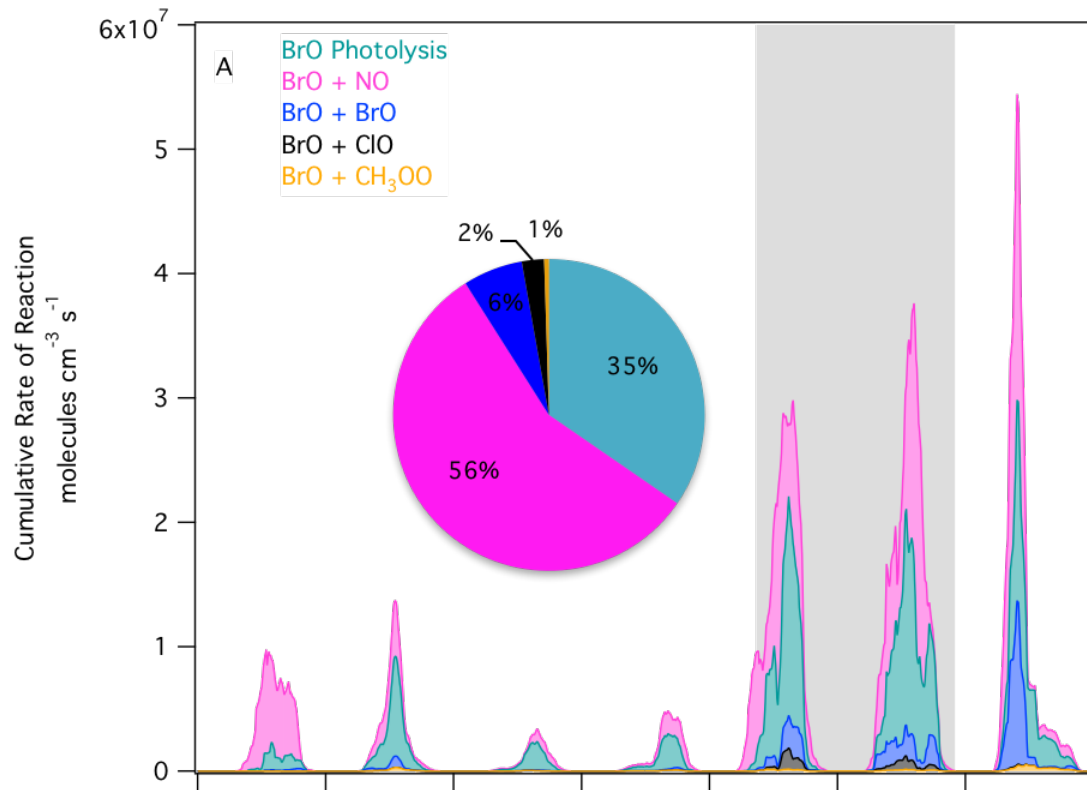
Fig 7. Time-varying rates of the most important bromine propagation reactions in the Base Model with Br and Cl present (Panel A) and with iodine included (Panel B). The BrO + BrO reaction is calculated as $2k[BrO]^2$ as this reaction regenerates two Br atoms. Model output is smoothed by hourly averaging. The y-axis is expressed as a cumulative rate of reaction. The grey shaded box represents a period of missing Br_2 observations. Time is expressed in Alaska Standard Time. The inset pie charts show the average fractional importance of each reaction pathway for only days 29 and 30 March (i.e. background O_3 days).
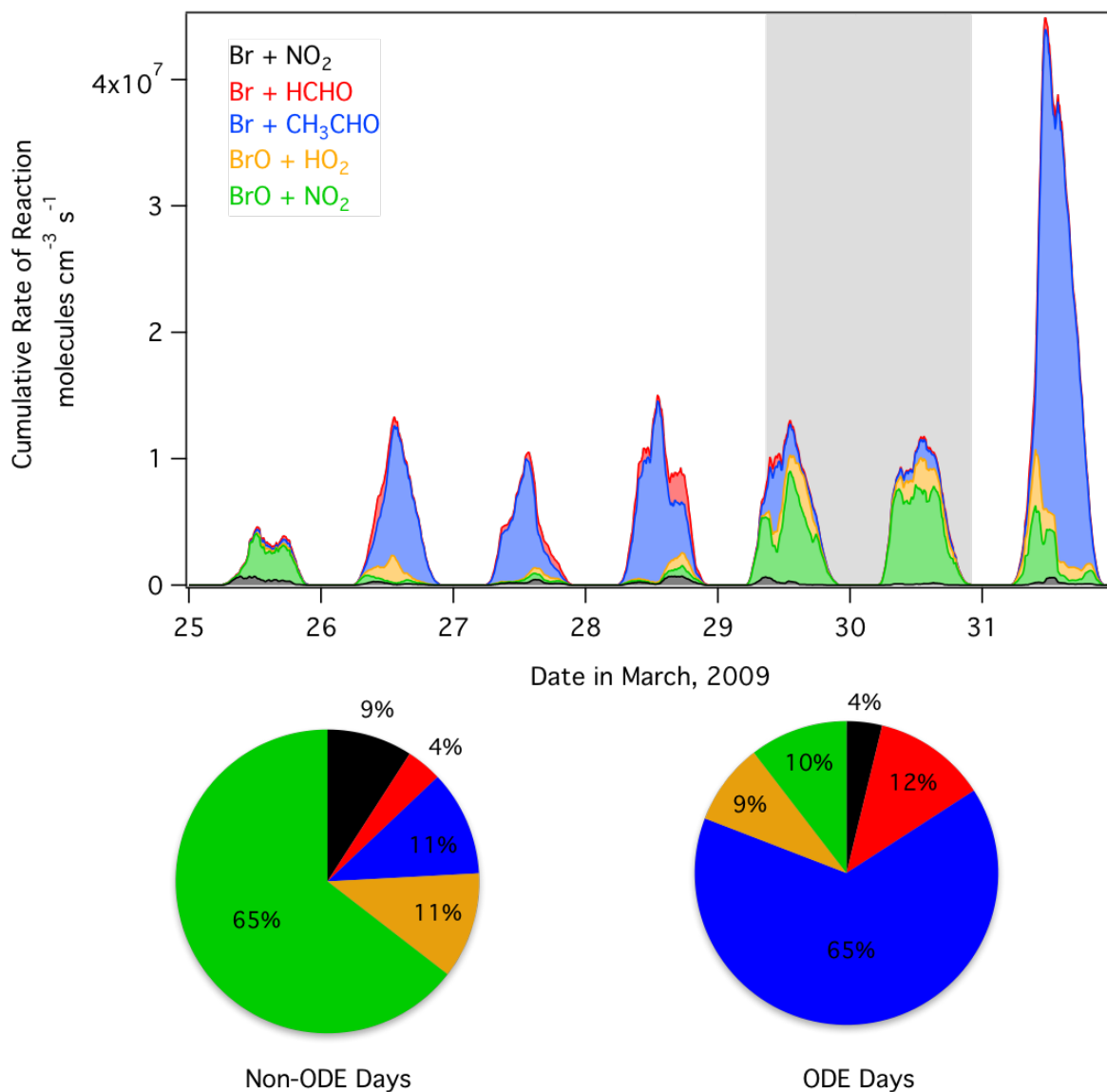
Fig 8. Time-varying rates of the most important reactive bromine (BrO_x) termination reactions in the Base Model. Model output is smoothed by hourly averaging. The y-axis is expressed as a cumulative rate of reaction. The grey shaded box represents a period of missing Br_2 observations. Time is expressed in Alaska Standard Time. The pie charts show the average fractional importance of each reactive bromine sink for non-ODE (background O_3) days and ODE days.

51

1267
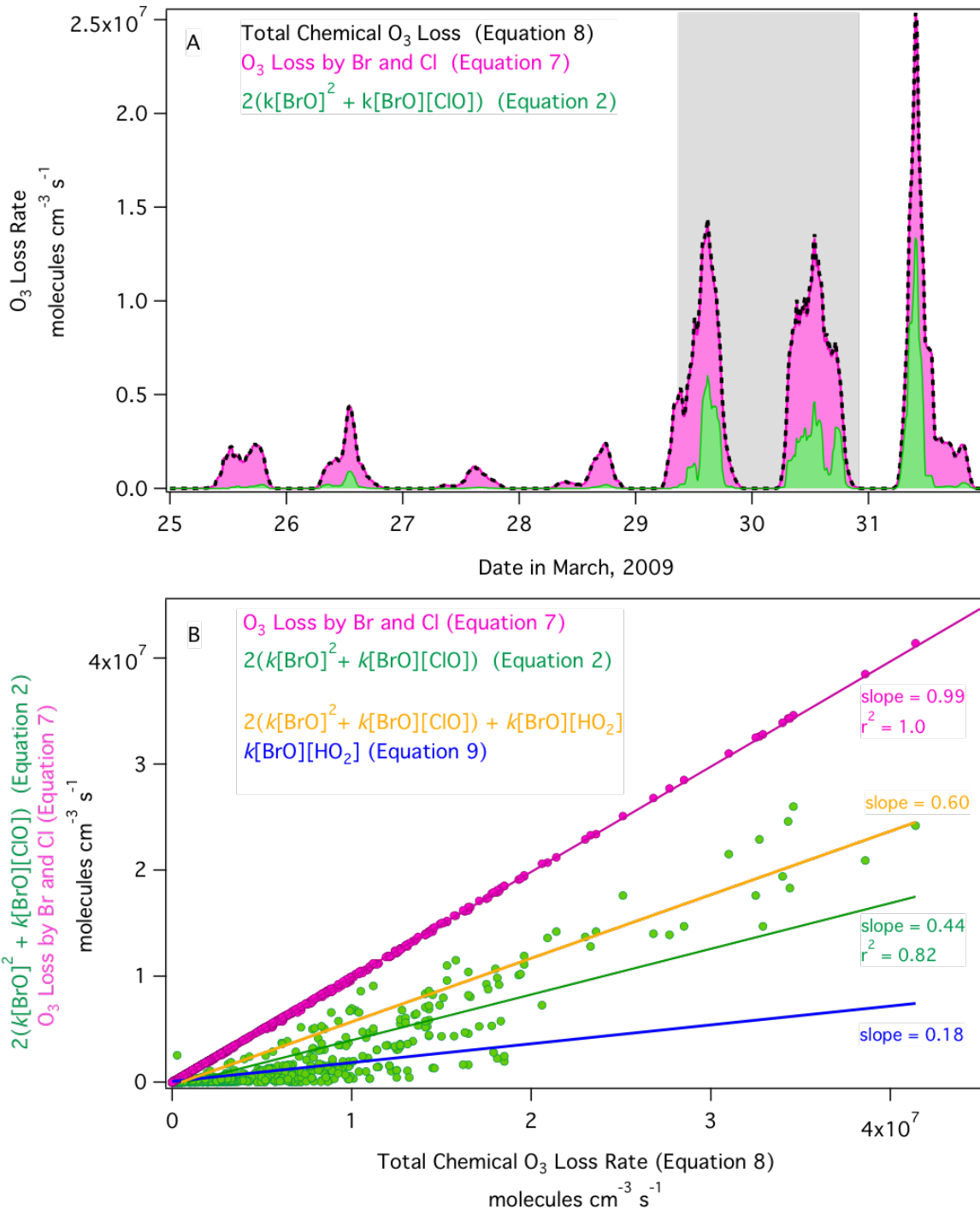
1268

1269 **Fig 9.** A) Comparison of the time-varying O_3 loss rate calculated using the estimation of
1270 $2(k[BrO]^2 + k[BrO][ClO])$ (Equation 2, green), the simulated O_3 loss rate by Br and Cl (Equation
1271 7, pink), and the total simulated chemical O_3 loss rate (Equation 8, dashed black trace). Model
1272 output is smoothed by hourly averaging. The grey shaded box represents a period of missing Br_2
1273 observations. Time is expressed in Alaska Standard Time. B) Shown is a regression of the

52

1274 $2(k[\text{BrO}]^2 + [\text{BrO}][\text{ClO}])$ <u>estimation method</u> (Equation 2) versus the total simulated chemical O_3

1275   loss rate in the Base Model (Equation 8) in the green data, and a regression of O_3 loss rate by Br

1276   and Cl only (Equation 7) versus the total simulated chemical O_3 loss rate in the pink data. <u>The</u>

1277   <u>blue trace represents the O_3 loss rate estimated by only considering $k[\text{BrO}][\text{HO}_2]$ (Equation 9).</u>

1278   <u>The orange trace estimates O_3 loss rate combining the three major gas-phase ozone depletion</u>

1279   <u>cycles.</u> The slopes represent the fraction of the chemical O_3 loss rate that can be accounted for by

1280   each method. For the conditions simulated, the commonly used estimation method of $2(k[\text{BrO}]^2$

1281 $+ [\text{BrO}][\text{ClO}])$ only accounts for 44% of the chemical O_3 loss rate.

1282
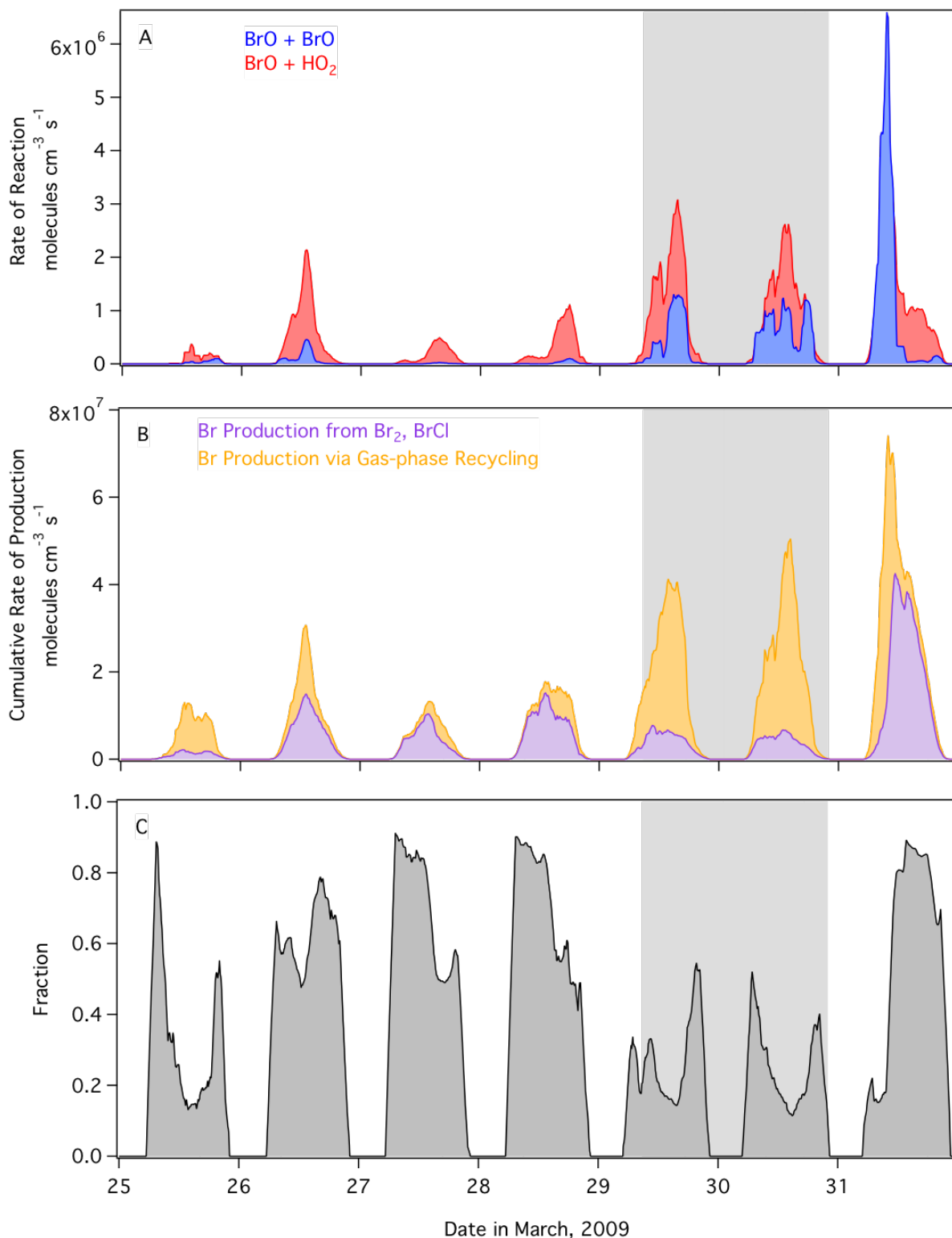
Fig 10. Panel A: Comparison of the rate of reaction of BrO + BrO (blue) and BrO + HO₂ (red). Panel B: The cumulative rate of Br atom production separated into the Br production rate from the photolysis of Br₂ and BrCl surface emissions calculated from Equation 10 (purple) and the Br

54

1287   atom production rate due to gas-phase radical recycling calculated from Equation 11 (orange).

1288   Panel C: The fraction of total Br atom production due to production from Br_2 and BrCl surface

1289   emissions. In all panels, model output is smoothed by hourly averaging. The grey shaded box

1290   represents a period of missing Br_2 observations. Time is expressed in Alaska Standard Time.

1291

1292